Reclaimed brick masonry waste recycling in macro-micro amelioration of cemented clayey soil: An eco-friendly construction waste solution

Ansar Ahmad [a], Usama Khalid [a], Zia ur Rehman [b,c,*], Muhammad Jawed Iqbal [a]

[a] National Institute of Transportation (NIT), Risalpur, National University of Sciences and Technology (NUST), Islamabad, 44000, Pakistan.

[b] School of Engineering, College of Science and Engineering, University of Derby, Derby DE22 3AW, UK

[c] School of Civil Engineering and Surveying, University of Portsmouth, Portland Building, Portland Street, Portsmouth, PO1 3AH, United Kingdom

[*]Corresponding Author
Email: engr.zrehman@gmail.com; ziaur.rehman@port.ac.uk

Abstract: Reclaimed brick masonry makes up a noteworthy portion of construction and demolition waste (CDW), totaling approximately 31%, even exceeding concrete waste. This study proposes using reclaimed brick masonry to enhance the micro and macro properties of clayey soil. Extensive laboratory testing was conducted to evaluate the performance of reclaimed brick powder (BP) along with 5% cement content. The cement was used to generate chemical bonds with BP and soil grains. Micro testing like XRF, XRD, EDAX, and SEM analyses confirmed the formation of CSH and CAH compounds which strengthened soil structure and enhanced its brittleness. However, after 10% BP, the addition of coarser grains converted the soil structure from dense to porous. Macro properties assessment confirmed that 10% BP with 5% cement content is an optimum combination for selected soil. The addition of BP reduces the required amount of cement for soil stabilization making it an eco-friendlier solution. The addition of the optimum combination decreased the w_L, I_P, FSI, w_{opt}, and C_c and increased the γ_{dmax}, q_u, CBR value, and σ_y significantly. It is also confirmed by the specimen's failure morphology analysis that BP with cement in clayey soil curtailed cement generated brittleness and enhanced ductility.

Keywords: Brick powder; clayey soil; cement; macro and micro properties; environmental implications

1. Introduction

The construction sector has a significant ecological footprint resulting from its extensive use of natural resources and the pollution generated throughout the processing and manufacturing stages [1-2]. Also, the eventual dismantling of infrastructures that have become superseded results in the sizeable generation of debris and waste. Construction and demolition waste (CDW) form a substantial fraction of the total waste produced, exceeding one-third of the overall waste generation [3]. Considering the generation of CDW in different parts of the globe, the United States generates nearly 534 MTPA of CDW, mainly through the deconstruction of structures, and likewise, CDW constitutes 30% to 40% of the total waste, amounting to around 1130 MTPA, in China, as depicted in Fig. 1, along some other densely populated countries. Natural disasters like floods, earthquakes, and tsunamis further add to the considerable volume of CDW, especially in developing countries because in developed countries, the core drivers of CDW generation are demolition and renovation activities and new construction. For instance, in Pakistan alone, earthquakes and floods have led to the destruction and damage of about 3.19 million and 1.88 million houses, respectively, over the past two decades, as presented in Fig. 2, along with some other structural damages [4]. Recent earthquakes in Syria and Turkiye caused the collapse of 9,100 and 273,000 buildings, respectively, as per the UNDP initial report. The CDW quantity will reach 2.59 billion tons by 2030, with an additional rise to 3.40 billion tons by 2050, as per World Bank projections [10].

To consider this issue seriously, developed countries are actively conducting extensive studies to address these challenges sustainably. Fig. 3 provides a depiction of the annual generation of CDW in various European countries, and the majority of these countries exhibit CDW recovery rates exceeding 90%, with the exceptions of Romania, the Slovak Republic, and Cyprus. Notably, some countries achieve CDW recovery rates of up to 100%. In contrast, the CDW recovery rate in mostly developing countries is very low. On the other hand, the construction sector is responsible for releasing 40% of CO_2 into the atmosphere and consumes 35% of the world's energy [11]. Furthermore, a Substantial proportion of CDW about 10% to 30%, of the total waste dumped in landfills on a global scale [12]. Consequently, there is growing interest among industry professionals and researchers in recycling CDW within the construction sector. This approach offers several advantages, including reduced carbon footprint, enhanced energy efficiency, supplementary economic benefits, and a reduction in the waste sent to landfills [13].

Brick masonry has been a primary construction material in various developed countries for the past several centuries [14]. However, with the ongoing process of massive modernization leading to the demolition of older infrastructure, the accumulation of waste brick masonry has been steadily rising [15]. Nevertheless, in developing countries, brick masonry remains a significant component in civil engineering construction, particularly in the construction of lightweight structures. It is worth noting that brick masonry constitutes a substantial portion of CDW, accounting for around 31% of the total CDW, surpassing the amount of concrete waste, as illustrated in Fig. 4. To employ waste brick masonry in an environmentally responsible manner, the optimal approach is to recycle this waste as a construction material. In several studies, reclaimed brick masonry is used in concrete as the replacement of coarse aggregates, fine aggregate, or cement and determined its impact on workability, mechanical properties, and microstructural properties of concrete [16-22]. Numerous studies have also been conducted to assess the effectiveness of crushed bricks as a component in unbound road layers, and reclaimed brick powder is being employed as an alternative filler in asphalt mixtures to improve the performance of the wearing course in flexible pavements [23-25]. Reclaimed brick powder (BP) is also used as a stabilizer to enhance the mechanical behavior of problematic soils and few studies have been focused on the physical properties and strength properties of BP-treated soils [14; 26-27]. To the best of the authors' knowledge, there is a lack of literature that delves into the microstructural attributes of soils treated with BP, employing methods like scanning electron microscopy (SEM) and energy-dispersive x-ray spectroscopy (EDAX) analyses. The efficacy of reclaimed brick masonry is inadequate to enhance the mechanical properties of construction materials alone up to the required limit, so, a huge amount of brick masonry is required to achieve the required outcomes from stabilization. To counter this issue, more chemically active additives like cement, lime, fly ash, bagasse ash, and alkaline activators can be used along with BP [14, 28].

In this study, reclaimed brick masonry is used in the form of powder to improve the macro (physical and mechanical) properties of clayey soil along some quantity of cement, because, in regions characterized by the presence of clayey soils, often referred to as 'hidden disaster' for structures due to their subpar macro properties [29]. In literature, it is found that BP acted as a pozzolanic material [30] and a key component in its chemical composition is SiO_2. Accordingly, its utilization with cement will enhance the pozzolanic competence of additives in soil because cement has a high percentage of CaO in its chemical composition. In this way, the combination of two additives can help to achieve the desired outcomes from treated clayey soils. The scope of this study is illustrated in Fig. 5. The impact of adding reclaimed brick powder (BP) and cement is assessed through physical and index properties such as consistency limits, free swell index, grain size distribution, and compaction properties. Unconfined compression tests and California bearing ratio tests are conducted on soil specimens treated with BP and cement, and with BP alone, to evaluate strength improvements. To assess the additive's efficacy on compression properties, 1D oedometer tests are performed. Microstructural tests, including scanning electron microscopy, energy-dispersive X-ray spectroscopy, and X-ray diffraction, are carried out to understand the improvement in macro properties of clayey soils.

2. Materials and methods

2.1. Materials characterization

2.1.1 Clayey soil

The clayey soil was collected in both disturbed and undisturbed states from Chokara, situated in Karak City, Pakistan. The geological composition of this area is predominantly characterized by alluvial deposits in the Indus River plain, featuring clayey deposits with varying levels of plasticity, spanning from low to high. The comprehensive geotechnical properties of the chosen soil are depicted in Fig. 6 and Table 1.

In Fig. 6a, the grain size distribution curve is illustrated, which was constructed based on the results of sieve and hydrometer analyses conducted by ASTM D7928 and D6913 standards, respectively. The analyses reveal that the selected soil consists of 48% clay, 49% silt, and 03% sand fractions. Notably, a substantial clay content, along with elevated values for both liquid limit (w_L) at 56.8% and plasticity index (I_P) at 33%, suggests the potential for significant soil shrinkage and swelling behavior. Consistency limits tests were carried out following the guidelines outlined in ASTM D4318. Based on the grain size distribution and consistency limits, the group symbol of soil has been categorized as CH with the group name of fat clay in accordance with the Unified Soil Classification System, following ASTM D2487. The results of standard and modified compaction test, unconfined compression test, and 1D oedometer test of selected soil were also presented in Figs. 6b, c, and d, respectively. Furthermore, x-ray fluorescence analysis was carried out to ascertain the soil's chemical composition. The analysis revealed the predominant oxides in the selected clay to be as follows: SiO_2 (65.87%), Al_2O_3 (9.71%), Fe_2O_3 (5.78%), and CaO (6.27%), as illustrated in Fig. 7a.

2.1.2 Additives

In this study, two additives, namely reclaimed brick masonry and cement, were employed to improve the overall geotechnical performance of clayey soil. Reclaimed brick masonry was employed in the form of reclaimed brick powder (BP). According to existing literature, the size of BP grains plays a critical role in achieving the desired outcomes [19]. For this study, grains of crushed reclaimed bricks smaller than 4.75 mm that passed through sieve no. 4 were designated as reclaimed BP. Considering the assertion made by Toledo Filho et al. [31] that cement mortar incorporating finer BP results in a denser microstructure and increased compressive strength, a decision was made in this study to opt for a coarser gradation of BP. This choice was made specifically for the clayey soil, which contains silt and clay grains, to promote the development of a denser soil structure. The grain size distribution of BP is illustrated in Fig. 6a. To accomplish this, reclaimed brick masonry was subjected to crushing in a Ball mill machine after the removal of any residual cement mortar. An analysis of the chemical composition revealed that the primary oxides present in the BP were as follows: SiO_2 (69.63%), Al_2O_3 (10.89%), and Fe_2O_3 (9.96%), as depicted in Fig. 7b. Additionally, a small quantity of ordinary Portland cement was used alongside the BP as an additive. The primary oxides in the chemical composition of cement, predominantly CaO, are displayed in Fig. 7c. Based on the chemical composition of all three materials, it becomes evident that when mixed in the presence of water, these materials possess the proficiency to generate cementitious substances known as calcium silicate hydrate (CSH) and calcium aluminate hydrate (CAH) compounds. These compounds serve to enhance the bonding among soil grains, thereby improving the macro properties of clayey soil.

2.2. Specimen preparation and methodology

2.2.1 Specimens remolding and tests matrix

To prepare the treated specimens for micro and macro properties evaluation, different proportions of reclaimed brick powder (BP) were employed as an additive, which was mixed with 5% cement. This percentage of cement was decided considering the concept of strength development rate with the increment of cement content in clayey soil, and usually, the boundary of the clay-cement interaction zone (Zone II) and the inactive zone (Zone I) starts from 5% of cement content, however; its value varies for clay to clay [32-33]. In general, 5%, 10%, 15%, and 20% BP were utilized in conjunction with 5% cement, nonetheless, certain unconfined compression tests were also conducted using only 5%, 10%, 15%, and 20% BP to assess BP's effectiveness in stabilizing clayey soil. The aforementioned tests were carried out on different specimens that incorporated BP and cement, and these specimens were allowed to cure for 7, 14, and 28 days. However, it's worth noting that the specific curing periods varied for each test. The test matrix for this study is provided in Table 2, and Fig. 8 illustrates the sample preparation process. For conducting ID consolidation tests, unconfined compression tests, and microstructural examinations like SEM and EDAX, the specimens were remodeled while adhering to standard compaction parameters, resulting in specimens with a height of 101.6 mm and a diameter of 50.8 mm. The specimens were subsequently resized according to the specific test requirements. On the other hand, for CBR tests, the specimens were remolded using modified compaction parameters. To ensure the maintenance of the required water content for the formation of the cementitious compounds, the remolded specimens were wrapped in polythene cling sheets and placed in a desiccator for curing, following recommendations from the literature [34].

2.2.2 Testing methods

2.2.2.1 Macro properties tests

The UCT assesses stress-strain behavior and undrained strength of soil specimens, adhering to ASTM D2166. This test evaluates the efficacy of treatments on clayey soils. Cylindrical specimens (50.8 mm diameter, 101.6 mm height) were used, with precise deformation measurements recorded by a high-precision displacement gauge. A consistent strain rate of 1 mm/min was maintained.

Unsoaked CBR tests, following ASTM D1883, assessed subgrade performance under applied loads. Specimens were remolded in 2315.5 cm^3 compaction molds using modified compaction parameters and cured for 7 and 28 days. Uniform compaction was ensured by evenly distributing blows. The tests used a 5 cm diameter plunger at a 1.3 mm/min penetration rate, with CBR values determined at 0.254 cm and 0.508 cm penetration depths.

Soil specimens underwent 1D consolidation tests with standard oedometers, following ASTM D2435. Specimens in 60 cm diameter, 20 mm height brass rings were saturated for 24 hours in the oedometer cell. Consolidation pressure was incrementally applied in six stages (49.94 kPa to 1598 kPa) and four unloading stages. Each stage's pressure was twice that of the previous and maintained for 24 hours. Parameters such as compression index (C_c), initial void ratio (e_0), and yield stress (σ_y) were derived from the compression curves to evaluate soil improvement.

2.2.2.2 Micro properties tests

To minimize potential microstructural disruptions, small specimens (approx. 125 mm^3) were sectioned using a scalpel for SEM and EDAX analyses after 28 days of curing. These specimens were air-dried to avoid fabric distortions from thermal stresses associated with oven drying. They were then placed on aluminum stubs with their surfaces facing upwards and shielded with conducting tape to prevent electrical charge accumulation. A thin gold layer was applied via ion sputter to enhance conductivity before SEM and EDAX analyses using a JEOL

JSM-IT100 with an energy-dispersive X-ray detector to determine surface composition. XRD analyses were also performed on treated and untreated specimens, transformed into a powdered form after 28 days of curing, to investigate chemical composition changes. Additionally, X-ray fluorescence analyses were conducted to ascertain the oxide composition of the soil, BP, and cement.

3. Test results and discussions

3.1. Micro properties of treated clayey soil

3.1.1 XRD analysis

Fig. 9 illustrates the mineralogical deviations observed in a 10% BP cum 5% cement-treated specimen in comparison to an untreated one of the same clayey soil. The curing period for the treated specimen was set at 28 days. The XRD analysis of untreated specimen reveals quartz as the primary mineral (Fig. 9a), with key peaks present at different 2θ angles, such as 22° and 26°. Meanwhile, significant alterations can be detected in the XRD pattern of the treated specimen, as shown in Fig. 9b. The increase in the height of the major peaks of quartz might be attributed to the addition of BP and cement. These additives primarily contain oxides such as CaO and SiO_2 alongside Al_2O_3. In the XRD pattern of the treated specimen, several additional minor peaks emerged due to the formation of cementitious compounds, namely calcium aluminate hydrate (CAH) and calcium silicate hydrate (CSH). These compounds result from the reactions between CaO with SiO_2 and Al_2O_3 in the presence of H_2O. In the proposed soil improvement approach, the development of multiple compounds, including CSH and CAH, binds the grains within the soil structure, rendering them more rigid and enhancing the macro properties of clayey soil [35].

3.1.2 EDAX analysis

Analysis using an energy-dispersive X-ray spectrometer (EDAX) was conducted to identify elemental changes in specimens treated with varying percentages of BP cum 5% cement content. The treated specimens were examined after 28 days of curing and contrasted with an untreated one of the same clayey soil. The EDAX spectrums of both treated and untreated specimens showcased dominant elements such as silicon (Si), calcium (Ca), aluminum (Al), iron (Fe), and magnesium (Mg) with notable peaks and relatively higher weight percentages (Fig. 10). It is evident that as the additive increases, there is a corresponding rise in the intensity of calcium peaks. This is attributed to the presence of CaO, one of the primary oxides in the chemical composition of the clayey soil and cement used (Fig. 7) [36].

Furthermore, the EDAX spectrum analyses reveal an abrupt increase in the Ca:Si and Ca:Al ratios as the BP content reaches up to 10% alongside the 5% cement content (Fig. 10b). The presence of Ca in the soil matrix, alongside Al and Si in the existence of water, assists the potential formation of CSH and CAH through chemical reactions among these elements [37]. Elevated levels of Ca compared to Al and Si, indicate enhanced development of cementitious compounds (CSH and CAH), as depicted in Fig. 10b. The growth in the Ca:Al and Ca:Si ratios diminished after reaching 10% BP due to the consistent percentage of cement content, as depicted in Figs. 10c and d. Based on both analyses presented in Figs. 7 and 10, it is evident that the proportion of Al in both soil and BP is lower than that of Si. Consequently, there's a likelihood that the quantity of CSH formed might exceed the formation of CAH. Additionally, the SEM images of the treated specimens confirmed the results obtained from EDAX. The formation of CSH and CAH compounds results from the hydration and pozzolanic reactions between soil, BP, and cement, leading to the creation of a relatively compact soil structure.

Additionally, these compounds contribute to improving the macro properties of treated clayey soil investigated in this study.

3.1.3 SEM analysis

Alterations in the microstructure of untreated specimens and those treated with BP cum cement were observed through scanning electron microscope (SEM) analysis. To enhance clarity of the microstructure in SEM images, Fig. 11 displays two SEM images for each specimen, taken at magnifications of 20µm and 50µm.

The SEM image of the untreated specimen exhibited a scattered and discontinuous microstructure, characterized by numerous medium to micropores and free silt particles larger than 20 µm, as especially shown in Fig. 11a-2. Moreover, the impact of any cementitious compounds on this soil structure cannot be discerned. According to Chen et al., [38], Pores within clayey soils are categorized by their sizes, namely macro-pores (ranging from 80 to 700 µm), medium pores (ranging from 2 to 80 µm), fine pores (ranging from 0.08 to 2 µm), and micropores (ranging from 0 to 0.08 µm).

The SEM images of specimens treated with 10% and 15% BP in combination with 5% cement revealed interconnected soil structures devoid of free silt particles (Figs. 11b and c). The silt particles were embraced into the soil structure due to the formation of cementitious compounds. Nonetheless, some medium to micropores are still discernible within these soil structures. Even, some sand grains larger than 50 µm can also be detected in Figs. 11b and c after the addition of BP content. In this study, the pozzolanic reaction between the SiO_2 and Al_2O_3 from BP and soil and $Ca(OH)_2$ from cement after hydration facilitated the generation of cementitious compounds such as CSH and CAH. The formation of the same cementitious compounds also discussed by [19], due to the reaction of cement and BP in concrete. It seems that the soil structure of the 10% BP-treated specimen is denser than the 15% BP-treated specimen, due to the presence of coarser grains in the 15% BP-treated specimen. This dense structure caused more brittleness and strength in the specimen treated with 10% BP and 5% cement as compared to other treated specimens.

3.2. Macro properties of treated clayey soil

3.2.1. Index properties

In Fig. 12, the impact of the addition of 5% cement along different percentages of BP on grain size distribution and fractions of different grains is discussed. With an increasing percentage of BP, the sand fraction increased as compared to the silt fraction. However, some increment in silt fraction was also noted. Meanwhile, the impact of the addition of BP on the clay fraction was significant. With an increasing percentage of BP, the clay fraction decreased considerably. Because, the major grains in grain size distribution of BP and clayey soil were sand and silt and silt and clay, respectively. So, with increasing the BP content in selected soil, clay fraction decreased and sand fraction increased but the effect of 5% BP along with 5% cement on fractions of silt, sand, and even clay was almost negligible due to the finer grains of cement.

The impact of varying percentages of BP along 5% cement on the liquid limit (w_L) and plasticity index (I_P) of clayey soil is depicted in Fig. 13a. As BP increased, both w_L and I_P decreased. This pattern remained prominent up to 10% BP; beyond this threshold, the alterations in these properties became negligible. Similar behavior of only BP-treated soil was also discussed by Blayi et al., [26]. Overall, there was a reduction of 32.2% in w_L and 65.6% in I_P, as the BP increased from 0 to 10% in soil along with 5% cement. This reaction can be ascribed to substituting clayey grains with non-plastic grains of BP. Additionally, the addition of cement results in a reduction in the adsorption of Ca^{2+} ions onto the surface of clay grains, thereby diminishing the repulsion between adjacent diffused double layers and promoting edge-to-face contact between successive clay layers [39]. Consequently, clay grains aggregate into larger clusters, leading to an increment in the plastic limit (w_P) with a reduction in both the

w_L and I_P. After reaching a 10% BP content, the alteration in w_L and I_P almost halted. This may be due to the transition phase which came after the 10% BP content with a combination of 5% cement. On the other hand, Fig. 13b illustrates the shift in the classification of clayey soil from CH (fat clay) to ML (low plastic silt). Because, the replacement of clayey grains with non-plastic coarser grains of BP results in a decrease in the repulsive forces among the soil grains, thereby encouraging grains agglomeration.

The free swell index (FSI) is defined as the percentage increase in the volume of clayey soil after it swells freely in water for a set period, typically 24 hours, using a dry and pulverized soil specimen for testing. FSI serves as a vital measure for assessing the volumetric behavior of clayey soils. Hence, to evaluate the effectiveness of the varying BP content with a combination of 5% cement content in addressing this issue, FSI tests were conducted on both untreated and treated specimens. The treated specimen exhibited a notable reduction in FSI compared to the untreated one (Fig. 14). The reduction in FSI is particularly rapid up to a 10% BP content; however, the rate of reduction slows significantly beyond this point. This improvement in FSI is attributed to the substitution of non-swelling materials like BP with clay grains. A reduction of about 40% in FSI is noted, as the BP increased from 0 to 10% in soil along with 5% cement content.

3.2.2. Compaction properties

Fig. 15 illustrates how the compaction properties of the treated clayey soil are affected by the variation of BP content with 5% cement content. As depicted in Fig. 15a, it is observed that as the percentage of additives increased, the peak points of the compaction curves also increased. A clear reduction can be observed in the optimum water content (w_{opt}) as the percentage of BP increased with 5% cement content, while the maximum dry unit weight (γ_{dmax}) demonstrated an opposite trend compared to w_{opt} with the incorporation of additive (Fig. 15b). With the addition of BP ranging from 0 to 10%, the γ_{dmax} value increased by approximately 7.15%, while the w_{opt} value decreased by 13.80%. Due to the addition of BP, a similar trend of compaction properties of clayey soils was also discussed [14, 19]. Upon reaching a 10% BP content, any further change in compaction properties effectively ceased. Due to the addition of BP in clayey soil, the non-plastic coarser BP grains replaced the clay grains which decreased the specific surface area and also reduced the need for water to lubricate the clayey grains for densification. Considering this, initially, the γ_{dmax} increased and the w_{opt} decreased due to the addition of BP along with cement. However, at higher BP content, the excessive presence of coarser BP grains in the soil constructs a porous soil structure that insignificantly reduces the unit weight, and enhances the water-holding capacity, as discussed in section 3.1.3. Furthermore, it is well established in the literature that adding cement to clayey soil also improves the γ_{dmax} and reduces w_{opt} due to aggregation of grains.

3.2.3. Strength properties

3.2.3.1 Stress-strain behavior

Fig. 16a depicts a comparison of stress-strain curves of specimens treated with various percentages of BP and a specimen treated with 5% cement content, following 7 days of curing periods. Natural clayey soils generally exhibit different stress-strain behaviors, often characterized as ductile, semi-brittle, and brittle. Typically, soils treated with additives tend to display these behaviors. The slope of the stress-strain curve of the 5% cement-treated specimen before the failure point is more than the BP-treated specimens at the same curing period. Moreover, the cement-treated specimen exhibited more strain-softening behavior than the BP-treated specimens. It can also be observed that the strain at failure (ε_f) of the cement-treated specimen is less than the BP-treated specimens. It means BP-treated specimens displayed ductile behavior as compared to cement-treated specimens, and the addition of BP in cement-treated clayey soil increased the ductility. Cementation compounds are generated due to a pozzolanic reaction between the SiO_2, Al_2O_3, and $Ca(OH)_2$ upon the addition of cement in clayey soil, and these compounds fill the pores and make the soil structure more dense and stiff. So, clayey soil after cement treatment showed brittle behavior. On the other hand, the addition of coarser grains of BP in clayey soil generated a porous structure which enhanced the ductility. However, at the initial stage, when both BP and cement are used together to enhance the macro properties of clayey soil, the porous soil structure develops due to coarser BP grains filled with cementitious compounds generated due to the addition of cement. While, in this study, at higher percentages of BP, the 5% cement is insufficient to fill the pores. Therefore, after 10% BP content, treated specimens showed relatively less brittle behavior than the others, as illustrated in Fig. 16b. As the curing period progressed, several changes occurred: the slope of stress-strain curves before the failure point increased, the strain-softening response intensified, and ε_f decreased, as depicted in Fig. 16c. This is primarily due to the time-sensitive nature of the chemical reaction, particularly the pozzolanic reaction that occurred due to the addition of cement with BP in clayey soil. This chemical reaction leads to the formation of cementitious compounds, which tightly bind the soil grains, thereby reducing soil ductility while enhancing strength.

3.2.3.2 unconfined compressive strength

Fig. 17 discusses the impact of varying proportions of BP and cement individually, as well as their combinations, on unconfined compressive strength (q_u). The curing period for BP and cement alone was set at 7 days, while specimens treated with BP cum cement content were tested considering the different curing periods, including 7, 14, and 28 days. The influence of BP on q_u is almost negligible after 7 days of curing. A little increment can be noted at 10% BP just due to the increase in the γ_{dmax} because, at 10% BP, the selected clayey soil has a denser soil structure as compared to other percentages. Further, there is no chemical reaction occurred between the BP and clayey soil to improve the strength as the SiO_2 and Al_2O_3 are the dominant oxides in both materials. The effect of 5% cement content on q_u is considerable as compared to BP, after 7 days of curing. The q_u of 5% and 10% BP-treated specimens is about 200% less than the q_u of 5% cement-treated specimen because there is a strong pozzolanic reaction between the oxides of cement and clayey soil which generates the CSH and CAH compounds to strengthen the soil structure. On the other hand, the addition of BP only influences the unit weight (γ) of soil.

The combined effect of BP and cement on the q_u is discussed in 2nd half of Fig. 17 considering the curing periods of 7, 14, and 28 days. Up to 10% BP addition in clayey soil along the cement, the q_u-values increased but later, these values decreased with increment of BP content. Because at higher BP content, the soil structure of clayey soil becomes porous due to sand and silt grains of BP. Also, cement content remains the same for all percentages of BP, so, the tendency of chemical reactions between the cement, soil, and BP oxides may also be compromised at higher percentages of BP. However, the impact of BP along cement on the q_u is almost insignificant. The q_u-values of BP cum cement-treated specimens are very high than the only BP-treated specimens. At 10% BP content and 7 days of curing, the q_u of only BP treated specimen is around 261% less than the BP cum cement treated specimen.

On the other hand, there is little difference between the q_u-values of the cement-treated specimen and BP cum cement-treated specimens. Since in the adopted approach of soil improvement, the addition of coarser grains of BP in clayey soil only impacts the γ of soil and this change has not a huge impact on strength properties. As compared to the untreated one, the q_u-values of treated specimens are very high. It is also worth noting that as the curing period increased, the values of q_u also significantly rose, as more cementitious bonds were formed over time.

3.2.3.3 Failure morphology analysis

Fig. 18 presents the failure morphology of untreated, cement-, and BP-treated specimens obtained from the unconfined compression test. The untreated specimen exhibited clear bulging without any failure plane, so, the value of shear failure angle (α) is also zero (Fig. 18a). The strain at failure (ε_f) of this specimen is very high with a value of about 11%. Overall, the ductile failure of this specimen can be considered considering the high value of ε_f and low value of α. The 5% cement-treated specimen has a vertical failure plane of $\alpha \approx 90^o$, as illustrated in Fig. 18b. The ε_f-value of this specimen is only 3.75%. This brittle failure of cement-treated specimens indicated the formation of CSH and CAH which strengthen the soil structure and make it brittle. Figs. 18c-e depicts the impact of different BP contents on failure morphology. Overall, these all specimens have inclined failure planes with different values of α and ε_f. The α-values of BP-treated specimens are less than the cement-treated specimens with greater ε_f-values. Considering the α, ε_f, and failure plane mode, these specimens showed semi-brittle to brittle failure. Because the addition of BP in selected clayey soil only influences the γ of the soil and after 10% BP, the presence of a large quantity of coarser BP grains in soil structure reduces the γ which causes to decrease the α and increase the ε_f (Fig. 18e).

Fig. 19 presents the failure morphology of specimens treated with different percentages of BP and 5% cement content. It can be detected that with increasing the BP content, the α-values decreased while the ε_f-values increased. Moreover, the transition of failure planes can also be observed from vertical to inclined with increasing the BP content. Because excessive presence of coarser grains (sand and silt) in soil structure of clayey soil makes it more porous and also decreases the brittleness generated due to the addition of cement in this study. So, the failure mode is semi-brittle to brittle at 15% and 20% BP contents. The impact of curing on failure morphology of 5% BP cum 5% cement-treated specimens is discussed in Fig. 20. Effect of the curing period is clear on the failure plans and the α-value. With increasing the curing from 7 to 28 days, the α-value changed from around 60^{o} to 90^{o,} and failure planes transited to vertical form inclined due to the growth of CAH and CSH compounds.

3.2.3.4 Subgrade strength

California bearing ratio (CBR) tests are conducted to assess the effectiveness of treated soil as subgrade material, and specimens are subjected to curing periods of 7 and 28 days to investigate the influence of additives on soil structure. In Fig. 21a, stress-penetration curves for untreated and BP cum cement-treated specimens are depicted, considering different curing times and additive contents. In all tested specimens, stress increases linearly with penetration. However, the stress value of treated specimens exceeds that of untreated ones for equivalent penetration values, until reaching 10% BP, after which this trend reversed.

Fig. 21b presents a comparison of the CBR values between untreated and treated specimens, considering variations in curing period and additive content. A well-defined increase in the CBR values is evident following the addition of BP along cement after 7 and 28 days of curing periods. Specifically, the CBR value of the treated specimen showed an approximately 260% upsurge compared to the untreated specimen, attributed to the inclusion of 10% BP and 5% cement as additives. After 10% BP, a major reduction in CBR values is noticed due to the reduction in the γ caused by the presence of a large amount of coarser grains of BP in soil structure. Furthermore, the influence of curing on the CBR values of treated specimens is noticeable. With the curing period increasing from 7 to 28 days, a distinct improvement of around 9% in CBR values is observed, attributed to the development of cementitious compounds in the form of CAH and CSH.

3.2.4. Compression properties

The 1D consolidation tests were conducted on both treated and untreated specimens to inspect compression behavior, focusing on the initial void ratio (e_0), yield stress (σ_y), and compression index (C_c) [41]. All treated specimens underwent testing after 28 days of the curing period, without considering the influence of curing on compression properties. A comparison of compression curves (e-logσ_v relationships) is depicted in Fig. 22a. In treated specimens, there is a small reduction observed in the void ratio in the pre-yield curve compared to untreated one (refer to Fig. 6d), attributable to the formation of cementitious compounds. However, a rapid decrease in the void ratio is noticeable in the post-yield curve due to the fracture of cementitious bonds under higher σ_v.

Figs. 22b and c illustrate the trends in e_0, σ_y, and C_c of various percentages of BP cum 5% cement-treated specimens. The e_0 and C_c exhibited an increase and the σ_y displayed a decrease of up to 10% BP, attributed to the introduction of densification due to BP and cementitious and reinforcing compounds into the soil structure, within acceptable limits. The continued enhancement in e_0, after 10% BP, is attributed to the surplus BP content, which impeded densification and led to the production of porous soil structure. The impact of this excess BP is relatively minor on C_c compared to σ_y, while σ_y displayed contrasting behavior after 10% BP. This change is attributed to void growth and a decrease in the γ [41–42].

4. Environmental and field implications

A significant allocation of resources is essential for implementing sustainable waste management strategies for CDW, posing a concerning challenge, particularly in developing nations. The generation of CDW is associated with numerous environmental and social issues, including a) squandering of resources encompassing labor, materials, and energy; b) aesthetic repercussions in case of mismanagement; c) health hazards for handlers; d) costs associated with the disposal of CDW; e) requirement for landfill space; f) pollution from hazardous materials: g) energy consumption in the management of CDW; h) climate change through greenhouse gas emissions. However, extensive research efforts are underway to address these challenges in sustainable ways. The prevalent method in modern construction involves recycling and repurposing CDW for the development of new infrastructure. CDW finds effective application across various infrastructure projects, serving as subbase and base materials, fill material, and replacing aggregates in both asphalt and concrete, among other uses [41-43].

Overall, CDW generation exceeds 3 billion tons around the world [45], and reclaimed brick masonry constitutes a substantial proportion of CDW, comprising around 31% of the total CDW [46]. So, a considerable quantity of reclaimed brick masonry is present within the CDW stream, suitable for utilization in construction projects. To implement this study in the field, it is crucial to assess the demand for reclaimed brick masonry based on the needs of the proposed soil improvement approach. To estimate the waste material required for soil improvement in a civil engineering project, the following Equation can be used as per [47-48].

$$\beta = \gamma A t \eta \quad (1)$$

where β is the amount of waste needed for soil improvement, γ is the unit weight of soil, A and t are the area and thickness of the soil, respectively and η is the optimized percentage of waste. The optimal macro properties of the treated clayey soil are attained with a 10% BP content in the proposed soil improvement approach. Taking this into account, for a two-lane road spanning 1 km, with a treated subgrade 0.5 m thick and 7 m wide, around 630 tons of BP would be necessary. Similarly, for a foundation covering an area of 150 m^2 with a treated subgrade layer 1 m thick, only 27 tons of BP would suffice (Fig. 23). Therefore, the availability of reclaimed brick masonry poses no obstacle to the implementation of the proposed soil improvement approach. A significant quantity of required CDW is accessible, and the proposed method shows promising potential in diverting a considerable amount of CDW away from landfills. Moreover, under field conditions, expansive clays necessitate a considerable quantity of cement ($\geq$ 15%) [49]. However, the current study demonstrates that a mere 5% cement, when combined with waste BP, proves adequate for soil stabilization. This demonstrates a substantial reduction in cement requirement which is traditionally the major and most convenient soil stabilizer due to logistical challenges associated with non-traditional cementing additives [50]. Consequently, the study proposes a practical approach to minimize cement usage in projects, addressing the current abundant usage of cement as the primary stabilizer. Thus, this study addresses waste management issues associated with CDW, contributing to waste recycling, pollution control, and sustainable industrial practices [51-52]. Additionally, it offers a practical approach to reducing cement demand for soil stabilization, thereby lowering the carbon footprint and mitigating global warming and other ecological issues [53].

5. Conclusions

This study introduces and assesses an approach to managing reclaimed brick masonry by combining it in the form of powder with cement to effectively improve the micro and macro properties of clayey soil. Through comprehensive macro and micro testing, this study yields the following key findings.

- For micro evaluation, XRF, XRD, EDAX, and SEM analyses were conducted, confirming the formation of cementitious compounds like CAH and CSH through reactions between CaO with SiO_2 and Al_2O_3 in the presence of H_2O. These compounds bonded grains together and filled pores in the soil structure, improving macro properties. SEM analysis also revealed that the soil structure of the 10% BP and 5% cement-treated specimen was denser compared to the 15% BP and 5% cement-treated specimen due to the excessive presence of coarser grains.

- As BP increased along the 5% cement content, physical and index properties like w_{opt}, FSI, $w_{L,}$ and I_P decreased, and the γ_{dmax} increased. This pattern remained prominent up to 10% BP; beyond this threshold, the alterations in these properties became negligible or less. Overall, there is a reduction of about 32.2% in w_L, 65.6% in I_P, 40% in FSA, and 13.80% in w_{opt} and an increment of around 7.15% in the γ_{dmax} as the BP increased from 0 to 10% in soil.
- The amelioration in the aforementioned properties is attributed to replacing clayey grains with non-plastic coarser BP grains which reduced the specific surface area and water lubrication needs for densification. Additionally, cement addition decreased Ca^{2+} ion adsorption on clay grain surfaces, decreasing repulsion between diffused double layers and promoting edge-to-face contact among clay layers, resulting in larger clusters and improved properties. However, beyond 10% BP content, excessive coarse BP grains created a porous soil structure, causing a reduction in unit weight and enhancement in water-holding capacity.
- The addition of BP in clayey soil has a lesser impact on q_u compared to cement. After 7 days of curing, the q_u of the 10% BP-treated specimen is about 200% lower than that of the 5% cement-treated specimen, as cement formed CSH and CAH compounds to strengthen the soil. However, BP primarily affects the soil's γ. Initially, up to 10% BP and 5% cement, q_u-values increased, but beyond this, they decreased due to the porous structure formed by higher BP content. Additionally, since cement content remains

constant for all BP percentages, chemical reaction tendencies may also be compromised.

- Failure morphology analysis revealed that cement-treated specimens exhibited a more brittle behavior than BP-treated specimens due to CAH and CSH compound generation, indicated by higher α-values and lower ε_f-values. Additionally, in BP cum 5% cement-treated specimens, as BP content increased, failure planes shifted from vertical to inclined, α-values decreased, and ε_f-values increased due to excessive coarse BP grains creating a more porous soil structure and reducing brittleness.
- The treated specimen exhibited a significant 260% increase in CBR value than the untreated one, ascribed to 10% BP and 5% cement inclusion. However, CBR values notably decreased after 10% BP due to a reduction in γ. Additionally, around 9% improvement in CBR values is observed with the increase in the curing period from 7 to 28 days, attributed to the development of cementitious compounds with time.
- The addition of various percentages of BP with 5% cement resulted in an increase in e_0 and C_c, and a decrease in σ_y up to 10% BP. Continued enhancement in e_0 after 10% BP is attributed to surplus BP content hindering densification. The impact of this excess BP is relatively minor on C_c compared to σ_y, which exhibits contrasting behavior after 10% BP due to a decrease in γ.

Declarations

Ethical approval

Not applicable

Consent to participate

Not applicable

Consent for publication

Not applicable

Availability of data and materials

The datasets used and/or analyzed during the current study are available from the corresponding author upon reasonable request.

Competing interests

The authors declare that they have no competing interests

Funding

Not applicable

Acknowledgment

NUST Risalpur is acknowledged for technical support.

References

[1] Huang B, Wang X, Kua H, Geng Y, Bleischwitz R, Ren J (2018) Construction and demolition waste management in China through the 3R principle. Resour Conserv Recycl 129: 36-44

[2] Barragan-Ramos A, Ríos-Fresneda C, Lizarazo-Marriaga J, Hernandez-Romero N (2022) Rebar corrosion and ASR durability assessment of fly ash concrete mixes using high contents of fine recycled aggregates. Constr Build Mater 349: 128759

[3] Gottsche J, Kelly M (2018) Assessing the impact of construction waste reduction on selected projects in Ireland. Waste Res Manag 171 (3): 71–81

[4] Hoang N H, Ishigaki T, Kubota R, Yamada M, Kawamoto K (2020) A review of construction and demolition waste management in Southeast Asia. J Mater Cycles Waste Manag 22(2): 315–325

[5] Haider H, Al Marshod S Y, Al Saleem S S, Ali A A M, Alinizzi M, Al Resheedi M T, Shafiquzzaman M (2022) Life cycle assessment of construction and demolition waste management in Riyadh, Saudi Arabia. Int J Environ Res Public Health 19(12): 7382

[6] Pereira P M, Vieira C S (2022) A literature review on the use of recycled construction and demolition materials in unbound pavement applications. Sustainability 14(21): 13918

[7] Swarna S K, Tezeswi T P, Kumar S M V N (2022) Implementing construction waste management in India: an extended theory of planned behaviour approach. Environ Technol Innov 27:102401

[8] ADB. Pakistan flood (2010): Preliminary damage and needs assessment. Asian Development Bank, November 2010

[9] European Environment Agency (EEA) (2020) ETC/WMGE Report 1/2020: construction and demolition waste: challenges and opportunities in a circular economy. European Environment Agency. 2020. Available online: https://www.eea.europa.eu/publications/construction-and-demolition-waste-challenges . 28 December 2024

[10] Guo H, Shi C, Guan X, Zhu J, Ding Y, Ling T-C (2018) Durability of recycled aggregate concrete - a review. Cem Concr Compos 89: 251–259
[11] Luangcharoenrat C, Intrachooto S, Peansupap V, Sutthinarakorn W (2019) Factors Influencing Construction Waste Generation in Building Construction: Thailand's Perspective. Sustainability 11(13): 3638
[12] Polat, A. Damci, H. Turkoglu, and A. P. Gurgun, (2017) Identification of Root Causes of Construction and Demolition (C&D) Waste: The Case of Turkey. Procedia Eng 196: 948-955
[13] Ghorbani B, Arulrajah A, Narsilio G, Horpibulsuk S (2020) Experimental and ANN analysis of temperature effects on the permanent deformation properties of demolition wastes. Transp Geotech 24: 100365
[14] Hidalgo C, Carvajal G, Muñoz F (2019) Laboratory evaluation of finely milled brick debris as a soil stabilizer. Sustainability 11(4) :967
[15] Zheng L, Ge Z, Yao Z, Gao Z (2011) Mechanical properties of mortar with recycled clay-brick-powder. ICCTP, ASCE 3379-3388
[16] Gonzalez J S, Gayarre F L, Perez C L, Ros P S, Serrano Lopez P S (2017) Influence of recycled brick aggregates on properties of structural concrete for manufacturing precast prestressed beams. Constr Build Mater 149: 507–514
[17] Baradaran-Nasiri A, Nematzadeh M (2017) The effect of elevated temperatures on the mechanical properties of concrete with fine recycled refractory brick aggregate and aluminate cement. Constr Build Mater 147: 865–875
[18] Nepomuceno M C S, Isidoro R A S, Catarino J P G (2018) Mechanical performance evaluation of concrete made with recycled ceramic coarse aggregates from industrial brick waste. Constr Build Mater 165: 284–294
[19] Dang J, Zhao J (2019) Influence of waste clay bricks as fine aggregate on the mechanical and microstructural properties of concrete. Constr Build Mater 228: 116757
[20] Rao M C (2021) Influence of brick dust, stone dust, and recycled fine aggregate on properties of natural and recycled aggregate concrete. Struct Concr 22: E105-E120
[21] Xu L, Su W, Su T (2022) Influence of recycled clay brick aggregate on the mechanical properties of concrete. Rev Adv Mater Sci 61: 372–380
[22] Chang J, Luo S-L, Ailifeila A, Chong L-L, Jiang J-Q (2022) Effects of coarse and fine crushed clay brick content on the compressive strength of recycled aggregate concrete and the microscopic mechanism. Geofluids 1341185
[23] Chen B, Zhu R, Chang F Z (2011a) Microstructural characteristics of volumetric deformation of clay under different compression stresses. Rock Soil Mech 32(1):95–100
[24] Wu S, Zhu J, Zhong J, Wang D (2011) Experimental investigation on related properties of asphalt mastic containing recycled red brick powder. Constr Build Mater 25(6): 2883–2887
[25] Arulrajah A, Perera S, Wong Y C, Horpibulsuk S, Maghool F (2020) Stiffness and flexural strength evaluation of cement stabilized PET blends with demolition wastes. Constr Build Mater 239: 117819
[26] Blayi R A, Sherwani F H, Ibrahim H H, Abdullah S J (2020) Stabilization of high-plasticity silt using waste brick powder. SN App Sci 2:1989
[27] Arifin Y F, Kusworo A S (2020) Utilization of lightweight brick waste as soils stabilizing agent. IOP Conf Series: Mater Sci Eng 980: 012071
[28] Ready S S, Prasad S C S V, Krishna N V (2018) Lime-stabilized black cotton soil and brick powder mixture as subbase material. Adv Civil Eng 5834685
[29] Ullah I, Khalid U, Rehman Z, Shah M M, Khan I, Ijaz N (2023) Integrated recycling of geopolymerized quarry dust and bagasse ash with facemasks for the balanced amelioration of the fat clay: a multi-waste solution. Environ Earth Sci 82: 516

[30] Mansoor S S, Hama S M, Hamdullah D N (2022) Effectiveness of replacing cement partially with waste brick powder in mortar. J King Soud Uni - Eng Sci. https://doi.org/10.1016/j.jksues.2022.01.004
[31] Toledo Filho R D, Gonçalves J P, Americano B B, Fairbairn E M R (2007) Potential for use of crushed waste calcined-clay brick as a supplementary cementitious material in Brazil. Cem Concr Res 37(9): 1357–1365
[32] Horpibulsuk S, Miura N, Nagaraj T S (2003) Assessment of strength development in cement-admixed at high water content clays with Abrams' law as a basis. Geotechnique 53(4): 439–444
[33] Khalid U, Liao C C, Ye G-L, Yadav S K (2018) Sustainable improvement of soft marine clay using low cement content: A multi-scale experimental investigation. Constr Build Mater 191: 469-480
[34] Phanikumar B R (2020) Silica fume stabilization of an expansive clay subgrade and the effect of silica fume-stabilised soil cushion on its CBR. Geomech Geoengin 15(1): 64–77
[35] Shah M M, Shahzad H M, Khalid U, Farooq K, Ur Rehman Z (2023) Experimental study on sustainable utilization of CKD for improvement of collapsible soil. Arab J Sci Eng 8: 5667–5682
[36] Yin Z-Y, Jin Y F, Shen S L, Huang H W (2016) An efficient optimization method for identifying parameters of soft structured clay by an enhanced genetic algorithm and elastic-viscoplastic model. Acta Geotech 12(4): 849–867
[37] Bilondi M P, Toufigh M M, Toufigh V (2018b Using calcium carbide residue as an alkaline activator for glass powdereclay geopolymer. Constr Build Mater 183:417–428
[38] Chen M-z, Lin J-t, Wu S-p, Liu C-h (2011) Utilization of recycled brick powder as alternative filler in asphalt mixture. Constr Build Mater 25(4):1532–1536
[39] Horpibulsuk S, Rachan R, Chinkulkijniwat A, Raksachon Y, Suddeepong A (2010) Analysis of strength development in cement-stabilized silty clay from microstructural considerations. Constr Build Mater 24: 2011–2021
[40] Rehman, Z. U., Khalid, U., Farooq, K., & Mujtaba, H. (2018). On yield stress of compacted clays. International Journal of Geo-Engineering, 9, 1-16.
[41] Khalid, U., Rehman, Z. U., Liao, C., Farooq, K., & Mujtaba, H. (2019). Compressibility of compacted clays mixed with a wide range of bentonite for engineered barriers. Arabian Journal for Science and Engineering, 44, 5027-5042.
[42] Wu, S., Cao, J., & Shao, Q. (2024). How to select remanufacturing mode: end-of-life or used product? Environment, Development and Sustainability. doi: https://doi.org/10.1007/s10668-024-04515-7
[43] Sattar, O., Khalid, U., Rehman, Z. U., Kayani, W. I., & Haider, A. (2024). Impact of crushing shape and geopolymerization on reclaimed concrete aggregate for recycling in the flexible pavement: An enhanced circular economy solution. Road Materials and Pavement Design, 25(9), 1910-1932.
[44] Mujtaba, H., Khalid, U., ur Rehman, Z., & Farooq, K. (2022). Recycling of reclaimed subbase materials in flexible pavement design. Road Materials and Pavement Design, 23(12), 2713-2732.
[45] Akhtar A, Sarmah A K (2018) Construction and demolition waste generation and properties of recycled aggregate concrete: A global perspective. J Clean Prodn 186: 262-281
[46] Mohammadinia A, Arulrajah A, Sanjayan J G, Disfani M M, Bo M W, Darmawan S (2016) Stabilization of demolition materials for pavement base/subbase applications using fly ash and slag geopolymers. J. Mater. Civ. Eng, 28 (7): 04016033

[47] ur Rehman, Z., & Khalid, U. (2021). Reuse of COVID-19 face mask for the amelioration of mechanical properties of fat clay: A novel solution to an emerging waste problem. Science of The Total Environment, 794, 148746.
[48] Rehman, Z. U., & Khalid, U. (2022). Optimization of COVID-19 face mask waste fibers and silica fume as a balanced mechanical ameliorator of fat clay using response surface methodology. Environmental Science and Pollution Research, 29(12), 17001-17016.
[49] Goodarzi, A. R., Akbari, H. R., & Salimi, M. J. A. C. S. (2016). Enhanced stabilization of highly expansive clays by mixing cement and silica fume. App Clay Sci, 132, 675-684.
[50] Zhao, H., Wang, Y., Liu, X., Wang, X., Chen, Z., Lei, Z.,... Singh, A. (2024). Review on solid wastes incorporated cementitious material using 3D concrete printing technology. Case Studies in Construction Materials, 21, e03676. doi: https://doi.org/10.1016/j.cscm.2024.e03676
[51] Liu, W., Zheng, J., Ou, X., Liu, X., Song, Y., Tian, C.,... Lin, Z. (2018). Effective Extraction of Cr(VI) from Hazardous Gypsum Sludge via Controlling the Phase Transformation and Chromium Species. Environmental Science & Technology, 52(22), 13336-13342. doi: https://doi.org/10.1021/acs.est.8b02213
[52] Liu, W., Li, J., Zheng, J., Song, Y., Shi, Z., Lin, Z.,... Chai, L. (2020). Different Pathways for Cr(III) Oxidation: Implications for Cr(VI) Reoccurrence in Reduced Chromite Ore Processing Residue. Environmental Science & Technology, 54(19), 11971-11979. doi: https://doi.org/10.1021/acs.est.0c01855
[53] Liu, X., Liu, X., & Zhang, Z. (2024). Application of red mud in carbon capture, utilization and storage (CCUS) technology. Renewable and Sustainable Energy Reviews, 202, 114683. doi: https://doi.org/10.1016/j.rser.2024.114683

List of Figures

Fig. 7. Oxides composition of (a) natural soil; (b) brick powder; (c) cement

Fig. 8. Specimens preparation approach

Fig. 9. XRD analyses of (a) untreated soil; (b) 5% cement+10% BP after 28 days of curing

Fig. 10. EDAX analyses of 5% cement treated specimens at 28 days curing (a) untreated soil; (b) 10% BP; (c) 15% BP; (d) 20% BP

Fig. 11. SEM images of 5% cement treated specimens at 28 days curing (a) untreated soil; (b) 10% BP; (c) 15% BP

Fig. 12. Effect of cement and BP on (a) grain size distribution curves; (b) effect of BP on grains fraction

Fig. 13. Effect of cement and BP on (a) consistency limits; (b) w_L vs. I_P

Fig. 14. Effect of cement and BP on FSI

Fig. 15. Effect of cement and BP on (a) compaction curves; (b) γ_{dmax} and w_{opt}

Fig. 16. Stress-strain curves of (a) cement and BP treated specimens; (b) effect of 5% cement+BP; (b) effect of curing

Fig. 17. Comparison of q_u of treated and untreated specimens

Fig. 18. Specimens failure morphology of (a) untreated; (b) 5% cement; (c) 5% BP; (d) 10% BP; (e) 20% BP

Fig. 19. Failure morphology of specimens treated with 5% cement and (a) 5% BP; (b) 10% BP; (c) 15% BP; (d) 20% BP, after 28 days of curing

Fig. 20. Failure morphology of specimens treated with 5% cement and 5% BP (a) 7 days; (b) 14 days; (c) 28 days

Fig. 21. CBR results (a) penetration vs σ curves; (b) effect of GFA and mellowing time; (c) effect of curing

Fig. 22. Effect of cement and BP on (a) compression parameters (b) σ_y and e_0; (b) C_c, after 28 days of curing

List of Tables

Nomenclatures

ASTM	American society for testing and materials
BP	Reclaimed brick powder
CAH	Calcium aluminate hydrate
CBR	California bearing ratio
CDW	Construction and demolition waste
CSH	Calcium silicate hydrate
C_c	Compression index
EDAX	Energy dispersive x-ray analysis
FSI	Free swell index
e	Void ratio
e_0	Initial void ratio
GSD	Grain size distribution
I_P	Plasticity index
q_u	Unconfined compressive strength
SEM	Scanning electron microscopy analysis
UCT	Unconfined compression test
USCS	Unified soil classification system
w	Water content
w_L	Liquid limit
w_n	Natural water content
w_{opt}	Optimum moisture content
w_P	Plastic limit
XRD	X-ray diffraction analysis
α	Shear failure angle
ε_a	Axial strain

ε_f	Strain at failure
γ	Unit weight
γ_d	Dry unit weight
γ_{dmax}	Maximum dry unit weight
σ	Stress
σ_v'	Effective vertical stress
σ_y	Yield stress

Reclaimed brick masonry waste recycling in macro-micro amelioration of cemented clayey soil: An eco-friendly construction waste solution

Ansar Ahmad [a], Usama Khalid [a], Zia ur Rehman [b,c,*], Muhammad Jawed Iqbal [a]

[a] National Institute of Transportation (NIT), Risalpur, National University of Sciences and Technology (NUST), Islamabad, 44000, Pakistan.

[b] School of Engineering, College of Science and Engineering, University of Derby, Derby DE22 3AW, UK

[c] School of Civil Engineering and Surveying, University of Portsmouth, Portland Building, Portland Street, Portsmouth, PO1 3AH, United Kingdom

[*]Corresponding Author
Email: engr.zrehman@gmail.com; ziaur.rehman@port.ac.uk

Abstract: Reclaimed brick masonry makes up a noteworthy portion of construction and demolition waste (CDW), totaling approximately 31%, even exceeding concrete waste. This study proposes using reclaimed brick masonry to enhance the micro and macro properties of clayey soil. Extensive laboratory testing was conducted to evaluate the performance of reclaimed brick powder (BP) along with 5% cement content. The cement was used to generate chemical bonds with BP and soil grains. Micro testing like XRF, XRD, EDAX, and SEM analyses confirmed the formation of CSH and CAH compounds which strengthened soil structure and enhanced its brittleness. However, after 10% BP, the addition of coarser grains converted the soil structure from dense to porous. Macro properties assessment confirmed that 10% BP with 5% cement content is an optimum combination for selected soil. The addition of BP reduces the required amount of cement for soil stabilization making it an eco-friendlier solution. The addition of the optimum combination decreased the w_L, I_P, FSI, w_{opt}, and C_c and increased the γ_{dmax}, q_u, CBR value, and σ_y significantly. It is also confirmed by the specimen's failure morphology analysis that BP with cement in clayey soil curtailed cement generated brittleness and enhanced ductility.

Keywords: Brick powder; clayey soil; cement; macro and micro properties; environmental implications

1. Introduction

The construction sector has a significant ecological footprint resulting from its extensive use of natural resources and the pollution generated throughout the processing and manufacturing stages [1-2]. Also, the eventual dismantling of infrastructures that have become superseded results in the sizeable generation of debris and waste. Construction and demolition waste (CDW) form a substantial fraction of the total waste produced, exceeding one-third of the overall waste generation [3]. Considering the generation of CDW in different parts of the globe, the United States generates nearly 534 MTPA of CDW, mainly through the deconstruction of structures, and likewise, CDW constitutes 30% to 40% of the total waste, amounting to around 1130 MTPA, in China, as depicted in Fig. 1, along some other densely populated countries. Natural disasters like floods, earthquakes, and tsunamis further add to the considerable volume of CDW, especially in developing countries because in developed countries, the core drivers of CDW generation are demolition and renovation activities and new construction. For instance, in Pakistan alone, earthquakes and floods have led to the destruction and damage of about 3.19 million and 1.88 million houses, respectively, over the past two decades, as presented in Fig. 2, along with some other structural damages [4]. Recent earthquakes in Syria and Turkiye caused the collapse of 9,100 and 273,000 buildings, respectively, as per the UNDP initial report. The CDW quantity will reach 2.59 billion tons by 2030, with an additional rise to 3.40 billion tons by 2050, as per World Bank projections [10].

To consider this issue seriously, developed countries are actively conducting extensive studies to address these challenges sustainably. Fig. 3 provides a depiction of the annual generation of CDW in various European countries, and the majority of these countries exhibit CDW recovery rates exceeding 90%, with the exceptions of Romania, the Slovak Republic, and Cyprus. Notably, some countries achieve CDW recovery rates of up to 100%. In contrast, the CDW recovery rate in mostly developing countries is very low. On the other hand, the construction sector is responsible for releasing 40% of CO_2 into the atmosphere and consumes 35% of the world's energy [11]. Furthermore, a Substantial proportion of CDW about 10% to 30%, of the total waste dumped in landfills on a global scale [12]. Consequently, there is growing interest among industry professionals and researchers in recycling CDW within the construction sector. This approach offers several advantages, including reduced carbon footprint, enhanced energy efficiency, supplementary economic benefits, and a reduction in the waste sent to landfills [13].

Brick masonry has been a primary construction material in various developed countries for the past several centuries [14]. However, with the ongoing process of massive modernization leading to the demolition of older infrastructure, the accumulation of waste brick masonry has been steadily rising [15]. Nevertheless, in developing countries, brick masonry remains a significant component in civil engineering construction, particularly in the construction of lightweight structures. It is worth noting that brick masonry constitutes a substantial portion of CDW, accounting for around 31% of the total CDW, surpassing the amount of concrete waste, as illustrated in Fig. 4. To employ waste brick masonry in an environmentally responsible manner, the optimal approach is to recycle this waste as a construction material. In several studies, reclaimed brick masonry is used in concrete as the replacement of coarse aggregates, fine aggregate, or cement and determined its impact on workability, mechanical properties, and microstructural properties of concrete [16-22]. Numerous studies have also been conducted to assess the effectiveness of crushed bricks as a component in unbound road layers, and reclaimed brick powder is being employed as an alternative filler in asphalt mixtures to improve the performance of the wearing course in flexible pavements [23-25]. Reclaimed brick powder (BP) is also used as a stabilizer to enhance the mechanical behavior of problematic soils and few studies have been focused on the physical properties and strength properties of BP-treated soils [14; 26-27]. To the best of the authors' knowledge, there is a lack of literature that delves into the microstructural attributes of soils treated with BP, employing methods like scanning electron microscopy (SEM) and energy-dispersive x-ray spectroscopy (EDAX) analyses. The efficacy of reclaimed brick masonry is inadequate to enhance the mechanical properties of construction materials alone up to the required limit, so, a huge amount of brick masonry is required to achieve the required outcomes from stabilization. To counter this issue, more chemically active additives like cement, lime, fly ash, bagasse ash, and alkaline activators can be used along with BP [14, 28].

In this study, reclaimed brick masonry is used in the form of powder to improve the macro (physical and mechanical) properties of clayey soil along some quantity of cement, because, in regions characterized by the presence of clayey soils, often referred to as 'hidden disaster' for structures due to their subpar macro properties [29]. In literature, it is found that BP acted as a pozzolanic material [30] and a key component in its chemical composition is SiO_2. Accordingly, its utilization with cement will enhance the pozzolanic competence of additives in soil because cement has a high percentage of CaO in its chemical composition. In this way, the combination of two additives can help to achieve the desired outcomes from treated clayey soils. The scope of this study is illustrated in Fig. 5. The impact of adding reclaimed brick powder (BP) and cement is assessed through physical and index properties such as consistency limits, free swell index, grain size distribution, and compaction properties. Unconfined compression tests and California bearing ratio tests are conducted on soil specimens treated with BP and cement, and with BP alone, to evaluate strength improvements. To assess the additive's efficacy on compression properties, 1D oedometer tests are performed. Microstructural tests, including scanning electron microscopy, energy-dispersive X-ray spectroscopy, and X-ray diffraction, are carried out to understand the improvement in macro properties of clayey soils.

2. Materials and methods

2.1. Materials characterization

2.1.1 Clayey soil

The clayey soil was collected in both disturbed and undisturbed states from Chokara, situated in Karak City, Pakistan. The geological composition of this area is predominantly characterized by alluvial deposits in the Indus River plain, featuring clayey deposits with varying levels of plasticity, spanning from low to high. The comprehensive geotechnical properties of the chosen soil are depicted in Fig. 6 and Table 1.

In Fig. 6a, the grain size distribution curve is illustrated, which was constructed based on the results of sieve and hydrometer analyses conducted by ASTM D7928 and D6913 standards, respectively. The analyses reveal that the selected soil consists of 48% clay, 49% silt, and 03% sand fractions. Notably, a substantial clay content, along with elevated values for both liquid limit (w_L) at 56.8% and plasticity index (I_P) at 33%, suggests the potential for significant soil shrinkage and swelling behavior. Consistency limits tests were carried out following the guidelines outlined in ASTM D4318. Based on the grain size distribution and consistency limits, the group symbol of soil has been categorized as CH with the group name of fat clay in accordance with the Unified Soil Classification System, following ASTM D2487. The results of standard and modified compaction test, unconfined compression test, and 1D oedometer test of selected soil were also presented in Figs. 6b, c, and d, respectively. Furthermore, x-ray fluorescence analysis was carried out to ascertain the soil's chemical composition. The analysis revealed the predominant oxides in the selected clay to be as follows: SiO_2 (65.87%), Al_2O_3 (9.71%), Fe_2O_3 (5.78%), and CaO (6.27%), as illustrated in Fig. 7a.

2.1.2 Additives

In this study, two additives, namely reclaimed brick masonry and cement, were employed to improve the overall geotechnical performance of clayey soil. Reclaimed brick masonry was employed in the form of reclaimed brick powder (BP). According to existing literature, the size of BP grains plays a critical role in achieving the desired outcomes [19]. For this study, grains of crushed reclaimed bricks smaller than 4.75 mm that passed through sieve no. 4 were designated as reclaimed BP. Considering the assertion made by Toledo Filho et al. [31] that cement mortar incorporating finer BP results in a denser microstructure and increased compressive strength, a decision was made in this study to opt for a coarser gradation of BP. This choice was made specifically for the clayey soil, which contains silt and clay grains, to promote the development of a denser soil structure. The grain size distribution of BP is illustrated in Fig. 6a. To accomplish this, reclaimed brick masonry was subjected to crushing in a Ball mill machine after the removal of any residual cement mortar. An analysis of the chemical composition revealed that the primary oxides present in the BP were as follows: SiO_2 (69.63%), Al_2O_3 (10.89%), and Fe_2O_3 (9.96%), as depicted in Fig. 7b. Additionally, a small quantity of ordinary Portland cement was used alongside the BP as an additive. The primary oxides in the chemical composition of cement, predominantly CaO, are displayed in Fig. 7c. Based on the chemical composition of all three materials, it becomes evident that when mixed in the presence of water, these materials possess the proficiency to generate cementitious substances known as calcium silicate hydrate (CSH) and calcium aluminate hydrate (CAH) compounds. These compounds serve to enhance the bonding among soil grains, thereby improving the macro properties of clayey soil.

2.2. Specimen preparation and methodology

2.2.1 Specimens remolding and tests matrix

To prepare the treated specimens for micro and macro properties evaluation, different proportions of reclaimed brick powder (BP) were employed as an additive, which was mixed with 5% cement. This percentage of cement was decided considering the concept of strength development rate with the increment of cement content in clayey soil, and usually, the boundary of the clay-cement interaction zone (Zone II) and the inactive zone (Zone I) starts from 5% of cement content, however; its value varies for clay to clay [32-33]. In general, 5%, 10%, 15%, and 20% BP were utilized in conjunction with 5% cement, nonetheless, certain unconfined compression tests were also conducted using only 5%, 10%, 15%, and 20% BP to assess BP's effectiveness in stabilizing clayey soil. The aforementioned tests were carried out on different specimens that incorporated BP and cement, and these specimens were allowed to cure for 7, 14, and 28 days. However, it's worth noting that the specific curing periods varied for each test. The test matrix for this study is provided in Table 2, and Fig. 8 illustrates the sample preparation process. For conducting ID consolidation tests, unconfined compression tests, and microstructural examinations like SEM and EDAX, the specimens were remodeled while adhering to standard compaction parameters, resulting in specimens with a height of 101.6 mm and a diameter of 50.8 mm. The specimens were subsequently resized according to the specific test requirements. On the other hand, for CBR tests, the specimens were remolded using modified compaction parameters. To ensure the maintenance of the required water content for the formation of the cementitious compounds, the remolded specimens were wrapped in polythene cling sheets and placed in a desiccator for curing, following recommendations from the literature [34].

2.2.2 Testing methods

2.2.2.1 Macro properties tests

The UCT assesses stress-strain behavior and undrained strength of soil specimens, adhering to ASTM D2166. This test evaluates the efficacy of treatments on clayey soils. Cylindrical specimens (50.8 mm diameter, 101.6 mm height) were used, with precise deformation measurements recorded by a high-precision displacement gauge. A consistent strain rate of 1 mm/min was maintained.

Unsoaked CBR tests, following ASTM D1883, assessed subgrade performance under applied loads. Specimens were remolded in 2315.5 cm^3 compaction molds using modified compaction parameters and cured for 7 and 28 days. Uniform compaction was ensured by evenly distributing blows. The tests used a 5 cm diameter plunger at a 1.3 mm/min penetration rate, with CBR values determined at 0.254 cm and 0.508 cm penetration depths.

Soil specimens underwent 1D consolidation tests with standard oedometers, following ASTM D2435. Specimens in 60 cm diameter, 20 mm height brass rings were saturated for 24 hours in the oedometer cell. Consolidation pressure was incrementally applied in six stages (49.94 kPa to 1598 kPa) and four unloading stages. Each stage's pressure was twice that of the previous and maintained for 24 hours. Parameters such as compression index (C_c), initial void ratio (e_0), and yield stress (σ_y) were derived from the compression curves to evaluate soil improvement.

2.2.2.2 Micro properties tests

To minimize potential microstructural disruptions, small specimens (approx. 125 mm^3) were sectioned using a scalpel for SEM and EDAX analyses after 28 days of curing. These specimens were air-dried to avoid fabric distortions from thermal stresses associated with oven drying. They were then placed on aluminum stubs with their surfaces facing upwards and shielded with conducting tape to prevent electrical charge accumulation. A thin gold layer was applied via ion sputter to enhance conductivity before SEM and EDAX analyses using a JEOL

JSM-IT100 with an energy-dispersive X-ray detector to determine surface composition. XRD analyses were also performed on treated and untreated specimens, transformed into a powdered form after 28 days of curing, to investigate chemical composition changes. Additionally, X-ray fluorescence analyses were conducted to ascertain the oxide composition of the soil, BP, and cement.

3. Test results and discussions

3.1. Micro properties of treated clayey soil

3.1.1 XRD analysis

Fig. 9 illustrates the mineralogical deviations observed in a 10% BP cum 5% cement-treated specimen in comparison to an untreated one of the same clayey soil. The curing period for the treated specimen was set at 28 days. The XRD analysis of untreated specimen reveals quartz as the primary mineral (Fig. 9a), with key peaks present at different 2θ angles, such as 22° and 26°. Meanwhile, significant alterations can be detected in the XRD pattern of the treated specimen, as shown in Fig. 9b. The increase in the height of the major peaks of quartz might be attributed to the addition of BP and cement. These additives primarily contain oxides such as CaO and SiO_2 alongside Al_2O_3. In the XRD pattern of the treated specimen, several additional minor peaks emerged due to the formation of cementitious compounds, namely calcium aluminate hydrate (CAH) and calcium silicate hydrate (CSH). These compounds result from the reactions between CaO with SiO_2 and Al_2O_3 in the presence of H_2O. In the proposed soil improvement approach, the development of multiple compounds, including CSH and CAH, binds the grains within the soil structure, rendering them more rigid and enhancing the macro properties of clayey soil [35].

3.1.2 EDAX analysis

Analysis using an energy-dispersive X-ray spectrometer (EDAX) was conducted to identify elemental changes in specimens treated with varying percentages of BP cum 5% cement content. The treated specimens were examined after 28 days of curing and contrasted with an untreated one of the same clayey soil. The EDAX spectrums of both treated and untreated specimens showcased dominant elements such as silicon (Si), calcium (Ca), aluminum (Al), iron (Fe), and magnesium (Mg) with notable peaks and relatively higher weight percentages (Fig. 10). It is evident that as the additive increases, there is a corresponding rise in the intensity of calcium peaks. This is attributed to the presence of CaO, one of the primary oxides in the chemical composition of the clayey soil and cement used (Fig. 7) [36].

Furthermore, the EDAX spectrum analyses reveal an abrupt increase in the Ca:Si and Ca:Al ratios as the BP content reaches up to 10% alongside the 5% cement content (Fig. 10b). The presence of Ca in the soil matrix, alongside Al and Si in the existence of water, assists the potential formation of CSH and CAH through chemical reactions among these elements [37]. Elevated levels of Ca compared to Al and Si, indicate enhanced development of cementitious compounds (CSH and CAH), as depicted in Fig. 10b. The growth in the Ca:Al and Ca:Si ratios diminished after reaching 10% BP due to the consistent percentage of cement content, as depicted in Figs. 10c and d. Based on both analyses presented in Figs. 7 and 10, it is evident that the proportion of Al in both soil and BP is lower than that of Si. Consequently, there's a likelihood that the quantity of CSH formed might exceed the formation of CAH. Additionally, the SEM images of the treated specimens confirmed the results obtained from EDAX. The formation of CSH and CAH compounds results from the hydration and pozzolanic reactions between soil, BP, and cement, leading to the creation of a relatively compact soil structure.

Additionally, these compounds contribute to improving the macro properties of treated clayey soil investigated in this study.

3.1.3 SEM analysis

Alterations in the microstructure of untreated specimens and those treated with BP cum cement were observed through scanning electron microscope (SEM) analysis. To enhance clarity of the microstructure in SEM images, Fig. 11 displays two SEM images for each specimen, taken at magnifications of 20μm and 50μm.

The SEM image of the untreated specimen exhibited a scattered and discontinuous microstructure, characterized by numerous medium to micropores and free silt particles larger than 20 μm, as especially shown in Fig. 11a-2. Moreover, the impact of any cementitious compounds on this soil structure cannot be discerned. According to Chen et al., [38], Pores within clayey soils are categorized by their sizes, namely macro-pores (ranging from 80 to 700 μm), medium pores (ranging from 2 to 80 μm), fine pores (ranging from 0.08 to 2 μm), and micropores (ranging from 0 to 0.08 μm).

The SEM images of specimens treated with 10% and 15% BP in combination with 5% cement revealed interconnected soil structures devoid of free silt particles (Figs. 11b and c). The silt particles were embraced into the soil structure due to the formation of cementitious compounds. Nonetheless, some medium to micropores are still discernible within these soil structures. Even, some sand grains larger than 50 μm can also be detected in Figs. 11b and c after the addition of BP content. In this study, the pozzolanic reaction between the SiO_2 and Al_2O_3 from BP and soil and $Ca(OH)_2$ from cement after hydration facilitated the generation of cementitious compounds such as CSH and CAH. The formation of the same cementitious compounds also discussed by [19], due to the reaction of cement and BP in concrete. It seems that the soil structure of the 10% BP-treated specimen is denser than the 15% BP-treated specimen, due to the presence of coarser grains in the 15% BP-treated specimen. This dense structure caused more brittleness and strength in the specimen treated with 10% BP and 5% cement as compared to other treated specimens.

3.2. Macro properties of treated clayey soil

3.2.1. Index properties

In Fig. 12, the impact of the addition of 5% cement along different percentages of BP on grain size distribution and fractions of different grains is discussed. With an increasing percentage of BP, the sand fraction increased as compared to the silt fraction. However, some increment in silt fraction was also noted. Meanwhile, the impact of the addition of BP on the clay fraction was significant. With an increasing percentage of BP, the clay fraction decreased considerably. Because, the major grains in grain size distribution of BP and clayey soil were sand and silt and silt and clay, respectively. So, with increasing the BP content in selected soil, clay fraction decreased and sand fraction increased but the effect of 5% BP along with 5% cement on fractions of silt, sand, and even clay was almost negligible due to the finer grains of cement.

The impact of varying percentages of BP along 5% cement on the liquid limit (w_L) and plasticity index (I_P) of clayey soil is depicted in Fig. 13a. As BP increased, both w_L and I_P decreased. This pattern remained prominent up to 10% BP; beyond this threshold, the alterations in these properties became negligible. Similar behavior of only BP-treated soil was also discussed by Blayi et al., [26]. Overall, there was a reduction of 32.2% in w_L and 65.6% in I_P, as the BP increased from 0 to 10% in soil along with 5% cement. This reaction can be ascribed to substituting clayey grains with non-plastic grains of BP. Additionally, the addition of cement results in a reduction in the adsorption of Ca^{2+} ions onto the surface of clay grains, thereby diminishing the repulsion between adjacent diffused double layers and promoting edge-to-face contact between successive clay layers [39]. Consequently, clay grains aggregate into larger clusters, leading to an increment in the plastic limit (w_P) with a reduction in both the

w_L and I_P. After reaching a 10% BP content, the alteration in w_L and I_P almost halted. This may be due to the transition phase which came after the 10% BP content with a combination of 5% cement. On the other hand, Fig. 13b illustrates the shift in the classification of clayey soil from CH (fat clay) to ML (low plastic silt). Because, the replacement of clayey grains with non-plastic coarser grains of BP results in a decrease in the repulsive forces among the soil grains, thereby encouraging grains agglomeration.

The free swell index (FSI) is defined as the percentage increase in the volume of clayey soil after it swells freely in water for a set period, typically 24 hours, using a dry and pulverized soil specimen for testing. FSI serves as a vital measure for assessing the volumetric behavior of clayey soils. Hence, to evaluate the effectiveness of the varying BP content with a combination of 5% cement content in addressing this issue, FSI tests were conducted on both untreated and treated specimens. The treated specimen exhibited a notable reduction in FSI compared to the untreated one (Fig. 14). The reduction in FSI is particularly rapid up to a 10% BP content; however, the rate of reduction slows significantly beyond this point. This improvement in FSI is attributed to the substitution of non-swelling materials like BP with clay grains. A reduction of about 40% in FSI is noted, as the BP increased from 0 to 10% in soil along with 5% cement content.

3.2.2. Compaction properties

Fig. 15 illustrates how the compaction properties of the treated clayey soil are affected by the variation of BP content with 5% cement content. As depicted in Fig. 15a, it is observed that as the percentage of additives increased, the peak points of the compaction curves also increased. A clear reduction can be observed in the optimum water content (w_{opt}) as the percentage of BP increased with 5% cement content, while the maximum dry unit weight (γ_{dmax}) demonstrated an opposite trend compared to w_{opt} with the incorporation of additive (Fig. 15b). With the addition of BP ranging from 0 to 10%, the γ_{dmax} value increased by approximately 7.15%, while the w_{opt} value decreased by 13.80%. Due to the addition of BP, a similar trend of compaction properties of clayey soils was also discussed [14, 19]. Upon reaching a 10% BP content, any further change in compaction properties effectively ceased. Due to the addition of BP in clayey soil, the non-plastic coarser BP grains replaced the clay grains which decreased the specific surface area and also reduced the need for water to lubricate the clayey grains for densification. Considering this, initially, the γ_{dmax} increased and the w_{opt} decreased due to the addition of BP along with cement. However, at higher BP content, the excessive presence of coarser BP grains in the soil constructs a porous soil structure that insignificantly reduces the unit weight, and enhances the water-holding capacity, as discussed in section 3.1.3. Furthermore, it is well established in the literature that adding cement to clayey soil also improves the γ_{dmax} and reduces w_{opt} due to aggregation of grains.

3.2.3. Strength properties

3.2.3.1 Stress-strain behavior

Fig. 16a depicts a comparison of stress-strain curves of specimens treated with various percentages of BP and a specimen treated with 5% cement content, following 7 days of curing periods. Natural clayey soils generally exhibit different stress-strain behaviors, often characterized as ductile, semi-brittle, and brittle. Typically, soils treated with additives tend to display these behaviors. The slope of the stress-strain curve of the 5% cement-treated specimen before the failure point is more than the BP-treated specimens at the same curing period. Moreover, the cement-treated specimen exhibited more strain-softening behavior than the BP-treated specimens. It can also be observed that the strain at failure (ε_f) of the cement-treated specimen is less than the BP-treated specimens. It means BP-treated specimens displayed ductile behavior as compared to cement-treated specimens, and the addition of BP in cement-treated clayey soil increased the ductility. Cementation compounds are generated due to a pozzolanic reaction between the SiO_2, Al_2O_3, and $Ca(OH)_2$ upon the addition of cement in clayey soil, and these compounds fill the pores and make the soil structure more dense and stiff. So, clayey soil after cement treatment showed brittle behavior. On the other hand, the addition of coarser grains of BP in clayey soil generated a porous structure which enhanced the ductility. However, at the initial stage, when both BP and cement are used together to enhance the macro properties of clayey soil, the porous soil structure develops due to coarser BP grains filled with cementitious compounds generated due to the addition of cement. While, in this study, at higher percentages of BP, the 5% cement is insufficient to fill the pores. Therefore, after 10% BP content, treated specimens showed relatively less brittle behavior than the others, as illustrated in Fig. 16b. As the curing period progressed, several changes occurred: the slope of stress-strain curves before the failure point increased, the strain-softening response intensified, and ε_f decreased, as depicted in Fig. 16c. This is primarily due to the time-sensitive nature of the chemical reaction, particularly the pozzolanic reaction that occurred due to the addition of cement with BP in clayey soil. This chemical reaction leads to the formation of cementitious compounds, which tightly bind the soil grains, thereby reducing soil ductility while enhancing strength.

3.2.3.2 unconfined compressive strength

Fig. 17 discusses the impact of varying proportions of BP and cement individually, as well as their combinations, on unconfined compressive strength (q_u). The curing period for BP and cement alone was set at 7 days, while specimens treated with BP cum cement content were tested considering the different curing periods, including 7, 14, and 28 days. The influence of BP on q_u is almost negligible after 7 days of curing. A little increment can be noted at 10% BP just due to the increase in the γ_{dmax} because, at 10% BP, the selected clayey soil has a denser soil structure as compared to other percentages. Further, there is no chemical reaction occurred between the BP and clayey soil to improve the strength as the SiO_2 and Al_2O_3 are the dominant oxides in both materials. The effect of 5% cement content on q_u is considerable as compared to BP, after 7 days of curing. The q_u of 5% and 10% BP-treated specimens is about 200% less than the q_u of 5% cement-treated specimen because there is a strong pozzolanic reaction between the oxides of cement and clayey soil which generates the CSH and CAH compounds to strengthen the soil structure. On the other hand, the addition of BP only influences the unit weight (γ) of soil.

The combined effect of BP and cement on the q_u is discussed in 2nd half of Fig. 17 considering the curing periods of 7, 14, and 28 days. Up to 10% BP addition in clayey soil along the cement, the q_u-values increased but later, these values decreased with increment of BP content. Because at higher BP content, the soil structure of clayey soil becomes porous due to sand and silt grains of BP. Also, cement content remains the same for all percentages of BP, so, the tendency of chemical reactions between the cement, soil, and BP oxides may also be compromised at higher percentages of BP. However, the impact of BP along cement on the q_u is almost insignificant. The q_u-values of BP cum cement-treated specimens are very high than the only BP-treated specimens. At 10% BP content and 7 days of curing, the q_u of only BP treated specimen is around 261% less than the BP cum cement treated specimen.

On the other hand, there is little difference between the q_u-values of the cement-treated specimen and BP cum cement-treated specimens. Since in the adopted approach of soil improvement, the addition of coarser grains of BP in clayey soil only impacts the γ of soil and this change has not a huge impact on strength properties. As compared to the untreated one, the q_u-values of treated specimens are very high. It is also worth noting that as the curing period increased, the values of q_u also significantly rose, as more cementitious bonds were formed over time.

3.2.3.3 Failure morphology analysis

Fig. 18 presents the failure morphology of untreated, cement-, and BP-treated specimens obtained from the unconfined compression test. The untreated specimen exhibited clear bulging without any failure plane, so, the value of shear failure angle (α) is also zero (Fig. 18a). The strain at failure (ε_f) of this specimen is very high with a value of about 11%. Overall, the ductile failure of this specimen can be considered considering the high value of ε_f and low value of α. The 5% cement-treated specimen has a vertical failure plane of $\alpha \approx 90^o$, as illustrated in Fig. 18b. The ε_f-value of this specimen is only 3.75%. This brittle failure of cement-treated specimens indicated the formation of CSH and CAH which strengthen the soil structure and make it brittle. Figs. 18c-e depicts the impact of different BP contents on failure morphology. Overall, these all specimens have inclined failure planes with different values of α and ε_f. The α-values of BP-treated specimens are less than the cement-treated specimens with greater ε_f-values. Considering the α, ε_f, and failure plane mode, these specimens showed semi-brittle to brittle failure. Because the addition of BP in selected clayey soil only influences the γ of the soil and after 10% BP, the presence of a large quantity of coarser BP grains in soil structure reduces the γ which causes to decrease the α and increase the ε_f (Fig. 18e).

Fig. 19 presents the failure morphology of specimens treated with different percentages of BP and 5% cement content. It can be detected that with increasing the BP content, the α-values decreased while the ε_f-values increased. Moreover, the transition of failure planes can also be observed from vertical to inclined with increasing the BP content. Because excessive presence of coarser grains (sand and silt) in soil structure of clayey soil makes it more porous and also decreases the brittleness generated due to the addition of cement in this study. So, the failure mode is semi-brittle to brittle at 15% and 20% BP contents. The impact of curing on failure morphology of 5% BP cum 5% cement-treated specimens is discussed in Fig. 20. Effect of the curing period is clear on the failure plans and the α-value. With increasing the curing from 7 to 28 days, the α-value changed from around 60^{o} to 90^{o}, and failure planes transited to vertical form inclined due to the growth of CAH and CSH compounds.

3.2.3.4 Subgrade strength

California bearing ratio (CBR) tests are conducted to assess the effectiveness of treated soil as subgrade material, and specimens are subjected to curing periods of 7 and 28 days to investigate the influence of additives on soil structure. In Fig. 21a, stress-penetration curves for untreated and BP cum cement-treated specimens are depicted, considering different curing times and additive contents. In all tested specimens, stress increases linearly with penetration. However, the stress value of treated specimens exceeds that of untreated ones for equivalent penetration values, until reaching 10% BP, after which this trend reversed.

Fig. 21b presents a comparison of the CBR values between untreated and treated specimens, considering variations in curing period and additive content. A well-defined increase in the CBR values is evident following the addition of BP along cement after 7 and 28 days of curing periods. Specifically, the CBR value of the treated specimen showed an approximately 260% upsurge compared to the untreated specimen, attributed to the inclusion of 10% BP and 5% cement as additives. After 10% BP, a major reduction in CBR values is noticed due to the reduction in the γ caused by the presence of a large amount of coarser grains of BP in soil structure. Furthermore, the influence of curing on the CBR values of treated specimens is noticeable. With the curing period increasing from 7 to 28 days, a distinct improvement of around 9% in CBR values is observed, attributed to the development of cementitious compounds in the form of CAH and CSH.

3.2.4. Compression properties

The 1D consolidation tests were conducted on both treated and untreated specimens to inspect compression behavior, focusing on the initial void ratio (e_0), yield stress (σ_y), and compression index (C_c) [40]. All treated specimens underwent testing after 28 days of the curing period, without considering the influence of curing on compression properties. A comparison of compression curves (e-logσ_v relationships) is depicted in Fig. 22a. In treated specimens, there is a small reduction observed in the void ratio in the pre-yield curve compared to untreated one (refer to Fig. 6d), attributable to the formation of cementitious compounds. However, a rapid decrease in the void ratio is noticeable in the post-yield curve due to the fracture of cementitious bonds under higher σ_v.

Figs. 22b and c illustrate the trends in e_0, σ_y, and C_c of various percentages of BP cum 5% cement-treated specimens. The e_0 and C_c exhibited an increase and the σ_y displayed a decrease of up to 10% BP, attributed to the introduction of densification due to BP and cementitious and reinforcing compounds into the soil structure, within acceptable limits. The continued enhancement in e_0, after 10% BP, is attributed to the surplus BP content, which impeded densification and led to the production of porous soil structure. The impact of this excess BP is relatively minor on C_c compared to σ_y, while σ_y displayed contrasting behavior after 10% BP. This change is attributed to void growth and a decrease in the γ [40–41].

4. Environmental and field implications

A significant allocation of resources is essential for implementing sustainable waste management strategies for CDW, posing a concerning challenge, particularly in developing nations. The generation of CDW is associated with numerous environmental and social issues, including a) squandering of resources encompassing labor, materials, and energy; b) aesthetic repercussions in case of mismanagement; c) health hazards for handlers; d) costs associated with the disposal of CDW; e) requirement for landfill space; f) pollution from hazardous materials: g) energy consumption in the management of CDW; h) climate change through greenhouse gas emissions. However, extensive research efforts are underway to address these challenges in sustainable ways. The prevalent method in modern construction involves recycling and repurposing CDW for the development of new infrastructure. CDW finds effective application across various infrastructure projects, serving as subbase and base materials, fill material, and replacing aggregates in both asphalt and concrete, among other uses [42-44].

Overall, CDW generation exceeds 3 billion tons around the world [45], and reclaimed brick masonry constitutes a substantial proportion of CDW, comprising around 31% of the total CDW [46]. So, a considerable quantity of reclaimed brick masonry is present within the CDW stream, suitable for utilization in construction projects. To implement this study in the field, it is crucial to assess the demand for reclaimed brick masonry based on the needs of the proposed soil improvement approach. To estimate the waste material required for soil improvement in a civil engineering project, the following Equation can be used as per [47-48].

$$\beta = \gamma A t \eta \quad (1)$$

where β is the amount of waste needed for soil improvement, γ is the unit weight of soil, A and t are the area and thickness of the soil, respectively and η is the optimized percentage of waste. The optimal macro properties of the treated clayey soil are attained with a 10% BP content in the proposed soil improvement approach. Taking this into account, for a two-lane road spanning 1 km, with a treated subgrade 0.5 m thick and 7 m wide, around 630 tons of BP would be necessary. Similarly, for a foundation covering an area of 150 m^2 with a treated subgrade layer 1 m thick, only 27 tons of BP would suffice (Fig. 23). Therefore, the availability of reclaimed brick masonry poses no obstacle to the implementation of the proposed soil improvement approach. A significant quantity of required CDW is accessible, and the proposed method shows promising potential in diverting a considerable amount of CDW away from landfills. Moreover, under field conditions, expansive clays necessitate a considerable quantity of cement (≥ 15%) [49]. However, the current study demonstrates that a mere 5% cement, when combined with waste BP, proves adequate for soil stabilization. This demonstrates a substantial reduction in cement requirement which is traditionally the major and most convenient soil stabilizer due to logistical challenges associated with non-traditional cementing additives [50]. Consequently, the study proposes a practical approach to minimize cement usage in projects, addressing the current abundant usage of cement as the primary stabilizer. Thus, this study addresses waste management issues associated with CDW, contributing to waste recycling, pollution control, and sustainable industrial practices [51-52]. Additionally, it offers a practical approach to reducing cement demand for soil stabilization, thereby lowering the carbon footprint and mitigating global warming and other ecological issues [53].

5. Conclusions

This study introduces and assesses an approach to managing reclaimed brick masonry by combining it in the form of powder with cement to effectively improve the micro and macro properties of clayey soil. Through comprehensive macro and micro testing, this study yields the following key findings.

- For micro evaluation, XRF, XRD, EDAX, and SEM analyses were conducted, confirming the formation of cementitious compounds like CAH and CSH through reactions between CaO with SiO_2 and Al_2O_3 in the presence of H_2O. These compounds bonded grains together and filled pores in the soil structure, improving macro properties. SEM analysis also revealed that the soil structure of the 10% BP and 5% cement-treated specimen was denser compared to the 15% BP and 5% cement-treated specimen due to the excessive presence of coarser grains.

- As BP increased along the 5% cement content, physical and index properties like w_{opt}, FSI, $w_{L,}$ and I_P decreased, and the γ_{dmax} increased. This pattern remained prominent up to 10% BP; beyond this threshold, the alterations in these properties became negligible or less. Overall, there is a reduction of about 32.2% in w_L, 65.6% in I_P, 40% in FSA, and 13.80% in w_{opt} and an increment of around 7.15% in the γ_{dmax} as the BP increased from 0 to 10% in soil.
- The amelioration in the aforementioned properties is attributed to replacing clayey grains with non-plastic coarser BP grains which reduced the specific surface area and water lubrication needs for densification. Additionally, cement addition decreased Ca^{2+} ion adsorption on clay grain surfaces, decreasing repulsion between diffused double layers and promoting edge-to-face contact among clay layers, resulting in larger clusters and improved properties. However, beyond 10% BP content, excessive coarse BP grains created a porous soil structure, causing a reduction in unit weight and enhancement in water-holding capacity.
- The addition of BP in clayey soil has a lesser impact on q_u compared to cement. After 7 days of curing, the q_u of the 10% BP-treated specimen is about 200% lower than that of the 5% cement-treated specimen, as cement formed CSH and CAH compounds to strengthen the soil. However, BP primarily affects the soil's γ. Initially, up to 10% BP and 5% cement, q_u-values increased, but beyond this, they decreased due to the porous structure formed by higher BP content. Additionally, since cement content remains

constant for all BP percentages, chemical reaction tendencies may also be compromised.

- Failure morphology analysis revealed that cement-treated specimens exhibited a more brittle behavior than BP-treated specimens due to CAH and CSH compound generation, indicated by higher α-values and lower ε_f-values. Additionally, in BP cum 5% cement-treated specimens, as BP content increased, failure planes shifted from vertical to inclined, α-values decreased, and ε_f-values increased due to excessive coarse BP grains creating a more porous soil structure and reducing brittleness.
- The treated specimen exhibited a significant 260% increase in CBR value than the untreated one, ascribed to 10% BP and 5% cement inclusion. However, CBR values notably decreased after 10% BP due to a reduction in γ. Additionally, around 9% improvement in CBR values is observed with the increase in the curing period from 7 to 28 days, attributed to the development of cementitious compounds with time.
- The addition of various percentages of BP with 5% cement resulted in an increase in e_0 and C_c, and a decrease in σ_y up to 10% BP. Continued enhancement in e_0 after 10% BP is attributed to surplus BP content hindering densification. The impact of this excess BP is relatively minor on C_c compared to σ_y, which exhibits contrasting behavior after 10% BP due to a decrease in γ.

Declarations

Ethical approval

Not applicable

Consent to participate

Not applicable

Consent for publication

Not applicable

Availability of data and materials

The datasets used and/or analyzed during the current study are available from the corresponding author upon reasonable request.

Competing interests

The authors declare that they have no competing interests

Funding

Not applicable

Acknowledgment

NUST Risalpur is acknowledged for technical support.

References

[1] Huang B, Wang X, Kua H, Geng Y, Bleischwitz R, Ren J (2018) Construction and demolition waste management in China through the 3R principle. Resour Conserv Recycl 129: 36-44

[2] Barragan-Ramos A, Ríos-Fresneda C, Lizarazo-Marriaga J, Hernandez-Romero N (2022) Rebar corrosion and ASR durability assessment of fly ash concrete mixes using high contents of fine recycled aggregates. Constr Build Mater 349: 128759

[3] Gottsche J, Kelly M (2018) Assessing the impact of construction waste reduction on selected projects in Ireland. Waste Res Manag 171 (3): 71–81

[4] Hoang N H, Ishigaki T, Kubota R, Yamada M, Kawamoto K (2020) A review of construction and demolition waste management in Southeast Asia. J Mater Cycles Waste Manag 22(2): 315–325

[5] Haider H, Al Marshod S Y, Al Saleem S S, Ali A A M, Alinizzi M, Al Resheedi M T, Shafiquzzaman M (2022) Life cycle assessment of construction and demolition waste management in Riyadh, Saudi Arabia. Int J Environ Res Public Health 19(12): 7382

[6] Pereira P M, Vieira C S (2022) A literature review on the use of recycled construction and demolition materials in unbound pavement applications. Sustainability 14(21): 13918

[7] Swarna S K, Tezeswi T P, Kumar S M V N (2022) Implementing construction waste management in India: an extended theory of planned behaviour approach. Environ Technol Innov 27:102401

[8] ADB. Pakistan flood (2010): Preliminary damage and needs assessment. Asian Development Bank, November 2010

[9] European Environment Agency (EEA) (2020) ETC/WMGE Report 1/2020: construction and demolition waste: challenges and opportunities in a circular economy. European Environment Agency. 2020. Available online: https://www.eea.europa.eu/publications/construction-and-demolition-waste-challenges . 28 December 2024

[10] Guo H, Shi C, Guan X, Zhu J, Ding Y, Ling T-C (2018) Durability of recycled aggregate concrete - a review. Cem Concr Compos 89: 251–259

[11] Luangcharoenrat C, Intrachooto S, Peansupap V, Sutthinarakorn W (2019) Factors Influencing Construction Waste Generation in Building Construction: Thailand’s Perspective. Sustainability 11(13): 3638

[12] Polat, A. Damci, H. Turkoglu, and A. P. Gurgun, (2017) Identification of Root Causes of Construction and Demolition (C&D) Waste: The Case of Turkey. Procedia Eng 196: 948-955

[13] Ghorbani B, Arulrajah A, Narsilio G, Horpibulsuk S (2020) Experimental and ANN analysis of temperature effects on the permanent deformation properties of demolition wastes. Transp Geotech 24: 100365

[14] Hidalgo C, Carvajal G, Muñoz F (2019) Laboratory evaluation of finely milled brick debris as a soil stabilizer. Sustainability 11(4) :967

[15] Zheng L, Ge Z, Yao Z, Gao Z (2011) Mechanical properties of mortar with recycled clay-brick-powder. ICCTP, ASCE 3379-3388

[16] Gonzalez J S, Gayarre F L, Perez C L, Ros P S, Serrano Lopez P S (2017) Influence of recycled brick aggregates on properties of structural concrete for manufacturing precast prestressed beams. Constr Build Mater 149: 507–514

[17] Baradaran-Nasiri A, Nematzadeh M (2017) The effect of elevated temperatures on the mechanical properties of concrete with fine recycled refractory brick aggregate and aluminate cement. Constr Build Mater 147: 865–875

[18] Nepomuceno M C S, Isidoro R A S, Catarino J P G (2018) Mechanical performance evaluation of concrete made with recycled ceramic coarse aggregates from industrial brick waste. Constr Build Mater 165: 284–294

[19] Dang J, Zhao J (2019) Influence of waste clay bricks as fine aggregate on the mechanical and microstructural properties of concrete. Constr Build Mater 228: 116757

[20] Rao M C (2021) Influence of brick dust, stone dust, and recycled fine aggregate on properties of natural and recycled aggregate concrete. Struct Concr 22: E105-E120

[21] Xu L, Su W, Su T (2022) Influence of recycled clay brick aggregate on the mechanical properties of concrete. Rev Adv Mater Sci 61: 372–380

[22] Chang J, Luo S-L, Ailifeila A, Chong L-L, Jiang J-Q (2022) Effects of coarse and fine crushed clay brick content on the compressive strength of recycled aggregate concrete and the microscopic mechanism. Geofluids 1341185

[23] Chen B, Zhu R, Chang F Z (2011a) Microstructural characteristics of volumetric deformation of clay under different compression stresses. Rock Soil Mech 32(1):95–100

[24] Wu S, Zhu J, Zhong J, Wang D (2011) Experimental investigation on related properties of asphalt mastic containing recycled red brick powder. Constr Build Mater 25(6): 2883–2887

[25] Arulrajah A, Perera S, Wong Y C, Horpibulsuk S, Maghool F (2020) Stiffness and flexural strength evaluation of cement stabilized PET blends with demolition wastes. Constr Build Mater 239: 117819

[26] Blayi R A, Sherwani F H, Ibrahim H H, Abdullah S J (2020) Stabilization of high-plasticity silt using waste brick powder. SN App Sci 2:1989

[27] Arifin Y F, Kusworo A S (2020) Utilization of lightweight brick waste as soils stabilizing agent. IOP Conf Series: Mater Sci Eng 980: 012071

[28] Ready S S, Prasad S C S V, Krishna N V (2018) Lime-stabilized black cotton soil and brick powder mixture as subbase material. Adv Civil Eng 5834685

[29] Ullah I, Khalid U, Rehman Z, Shah M M, Khan I, Ijaz N (2023) Integrated recycling of geopolymerized quarry dust and bagasse ash with facemasks for the balanced amelioration of the fat clay: a multi-waste solution. Environ Earth Sci 82: 516

[30] Mansoor S S, Hama S M, Hamdullah D N (2022) Effectiveness of replacing cement partially with waste brick powder in mortar. J King Soud Uni - Eng Sci. https://doi.org/10.1016/j.jksues.2022.01.004

[31] Toledo Filho R D, Gonçalves J P, Americano B B, Fairbairn E M R (2007) Potential for use of crushed waste calcined-clay brick as a supplementary cementitious material in Brazil. Cem Concr Res 37(9): 1357–1365

[32] Horpibulsuk S, Miura N, Nagaraj T S (2003) Assessment of strength development in cement-admixed at high water content clays with Abrams' law as a basis. Geotechnique 53(4): 439–444

[33] Khalid U, Liao C C, Ye G-L, Yadav S K (2018) Sustainable improvement of soft marine clay using low cement content: A multi-scale experimental investigation. Constr Build Mater 191: 469-480

[34] Phanikumar B R (2020) Silica fume stabilization of an expansive clay subgrade and the effect of silica fume-stabilised soil cushion on its CBR. Geomech Geoengin 15(1): 64–77

[35] Shah M M, Shahzad H M, Khalid U, Farooq K, Ur Rehman Z (2023) Experimental study on sustainable utilization of CKD for improvement of collapsible soil. Arab J Sci Eng 8: 5667–5682

[36] Yin Z-Y, Jin Y F, Shen S L, Huang H W (2016) An efficient optimization method for identifying parameters of soft structured clay by an enhanced genetic algorithm and elastic-viscoplastic model. Acta Geotech 12(4): 849–867

[37] Bilondi M P, Toufigh M M, Toufigh V (2018b Using calcium carbide residue as an alkaline activator for glass powdereclay geopolymer. Constr Build Mater 183:417–428

[38] Chen M-z, Lin J-t, Wu S-p, Liu C-h (2011) Utilization of recycled brick powder as alternative filler in asphalt mixture. Constr Build Mater 25(4):1532–1536

[39] Horpibulsuk S, Rachan R, Chinkulkijniwat A, Raksachon Y, Suddeepong A (2010) Analysis of strength development in cement-stabilized silty clay from microstructural considerations. Constr Build Mater 24: 2011–2021

[40] Rehman, Z. U., Khalid, U., Farooq, K., & Mujtaba, H. (2018). On yield stress of compacted clays. International Journal of Geo-Engineering, 9, 1-16.

[41] Khalid, U., Rehman, Z. U., Liao, C., Farooq, K., & Mujtaba, H. (2019). Compressibility of compacted clays mixed with a wide range of bentonite for engineered barriers. Arabian Journal for Science and Engineering, 44, 5027-5042.

[42] Wu, S., Cao, J., & Shao, Q. (2024). How to select remanufacturing mode: end-of-life or used product? Environment, Development and Sustainability. doi: https://doi.org/10.1007/s10668-024-04515-7

[43] Sattar, O., Khalid, U., Rehman, Z. U., Kayani, W. I., & Haider, A. (2024). Impact of crushing shape and geopolymerization on reclaimed concrete aggregate for recycling in the flexible pavement: An enhanced circular economy solution. Road Materials and Pavement Design, 25(9), 1910-1932.

[44] Mujtaba, H., Khalid, U., ur Rehman, Z., & Farooq, K. (2022). Recycling of reclaimed subbase materials in flexible pavement design. Road Materials and Pavement Design, 23(12), 2713-2732.

[45] Akhtar A, Sarmah A K (2018) Construction and demolition waste generation and properties of recycled aggregate concrete: A global perspective. J Clean Prodn 186: 262-281

[46] Mohammadinia A, Arulrajah A, Sanjayan J G, Disfani M M, Bo M W, Darmawan S (2016) Stabilization of demolition materials for pavement base/subbase applications using fly ash and slag geopolymers. J. Mater. Civ. Eng, 28 (7): 04016033

[47] ur Rehman, Z., & Khalid, U. (2021). Reuse of COVID-19 face mask for the amelioration of mechanical properties of fat clay: A novel solution to an emerging waste problem. Science of The Total Environment, 794, 148746.

[48] Rehman, Z. U., & Khalid, U. (2022). Optimization of COVID-19 face mask waste fibers and silica fume as a balanced mechanical ameliorator of fat clay using response surface methodology. Environmental Science and Pollution Research, 29(12), 17001-17016.

[49] Goodarzi, A. R., Akbari, H. R., & Salimi, M. J. A. C. S. (2016). Enhanced stabilization of highly expansive clays by mixing cement and silica fume. App Clay Sci, 132, 675-684.

[50] Zhao, H., Wang, Y., Liu, X., Wang, X., Chen, Z., Lei, Z.,... Singh, A. (2024). Review on solid wastes incorporated cementitious material using 3D concrete printing technology. Case Studies in Construction Materials, 21, e03676. doi: https://doi.org/10.1016/j.cscm.2024.e03676

[51] Liu, W., Zheng, J., Ou, X., Liu, X., Song, Y., Tian, C.,... Lin, Z. (2018). Effective Extraction of Cr(VI) from Hazardous Gypsum Sludge via Controlling the Phase Transformation and Chromium Species. Environmental Science & Technology, 52(22), 13336-13342. doi: https://doi.org/10.1021/acs.est.8b02213

[52] Liu, W., Li, J., Zheng, J., Song, Y., Shi, Z., Lin, Z.,... Chai, L. (2020). Different Pathways for Cr(III) Oxidation: Implications for Cr(VI) Reoccurrence in Reduced Chromite Ore Processing Residue. Environmental Science & Technology, 54(19), 11971-11979. doi: https://doi.org/10.1021/acs.est.0c01855

[53] Liu, X., Liu, X., & Zhang, Z. (2024). Application of red mud in carbon capture, utilization and storage (CCUS) technology. Renewable and Sustainable Energy Reviews, 202, 114683. doi: https://doi.org/10.1016/j.rser.2024.114683

List of Figures

Fig. 7. Oxides composition of (a) natural soil; (b) brick powder; (c) cement

Fig. 8. Specimens preparation approach

Fig. 9. XRD analyses of (a) untreated soil; (b) 5% cement+10% BP after 28 days of curing

Fig. 10. EDAX analyses of 5% cement treated specimens at 28 days curing (a) untreated soil; (b) 10% BP; (c) 15% BP; (d) 20% BP

Fig. 11. SEM images of 5% cement treated specimens at 28 days curing (a) untreated soil; (b) 10% BP; (c) 15% BP

Fig. 12. Effect of cement and BP on (a) grain size distribution curves; (b) effect of BP on grains fraction

Fig. 13. Effect of cement and BP on (a) consistency limits; (b) w_L vs. I_P

Fig. 14. Effect of cement and BP on FSI

Fig. 15. Effect of cement and BP on (a) compaction curves; (b) γ_{dmax} and w_{opt}

Fig. 16. Stress-strain curves of (a) cement and BP treated specimens; (b) effect of 5% cement+BP; (b) effect of curing

Fig. 17. Comparison of q_u of treated and untreated specimens

Fig. 18. Specimens failure morphology of (a) untreated; (b) 5% cement; (c) 5% BP; (d) 10% BP; (e) 20% BP

Fig. 19. Failure morphology of specimens treated with 5% cement and (a) 5% BP; (b) 10% BP; (c) 15% BP; (d) 20% BP, after 28 days of curing

Fig. 20. Failure morphology of specimens treated with 5% cement and 5% BP (a) 7 days; (b) 14 days; (c) 28 days

Fig. 21. CBR results (a) penetration vs σ curves; (b) effect of GFA and mellowing time; (c) effect of curing

Fig. 22. Effect of cement and BP on (a) compression parameters (b) σ_y and e_0; (b) C_c, after 28 days of curing

Fig. 23. CDW estimation for proposed soil improvement approach

List of Tables

Nomenclatures

ASTM	American society for testing and materials
BP	Reclaimed brick powder
CAH	Calcium aluminate hydrate
CBR	California bearing ratio
CDW	Construction and demolition waste
CSH	Calcium silicate hydrate
C_c	Compression index
EDAX	Energy dispersive x-ray analysis
FSI	Free swell index
e	Void ratio
e_0	Initial void ratio
GSD	Grain size distribution
I_P	Plasticity index
q_u	Unconfined compressive strength
SEM	Scanning electron microscopy analysis
UCT	Unconfined compression test
USCS	Unified soil classification system
w	Water content
w_L	Liquid limit
w_n	Natural water content
w_{opt}	Optimum moisture content
w_P	Plastic limit
XRD	X-ray diffraction analysis
α	Shear failure angle
ε_a	Axial strain

ε_f	Strain at failure
γ	Unit weight
γ_d	Dry unit weight
γ_{dmax}	Maximum dry unit weight
σ	Stress
σ_v'	Effective vertical stress
σ_y	Yield stress

Figure

Graphical Abstract

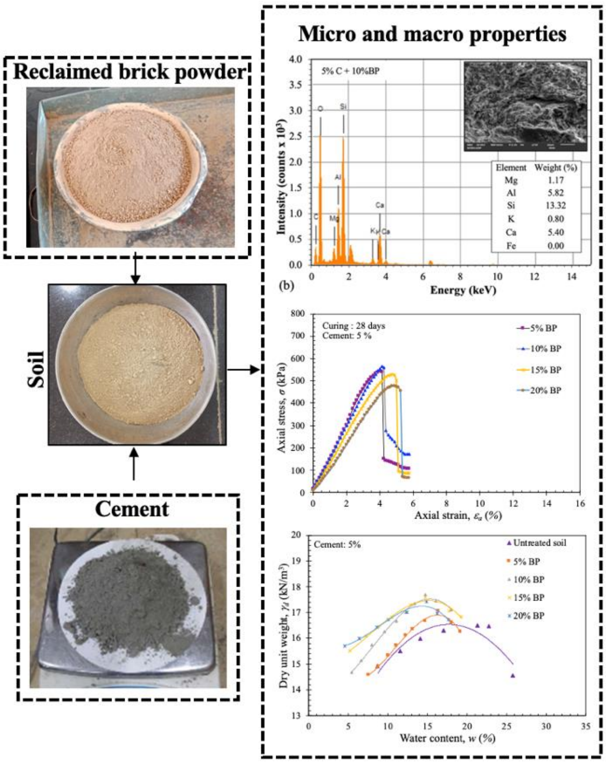

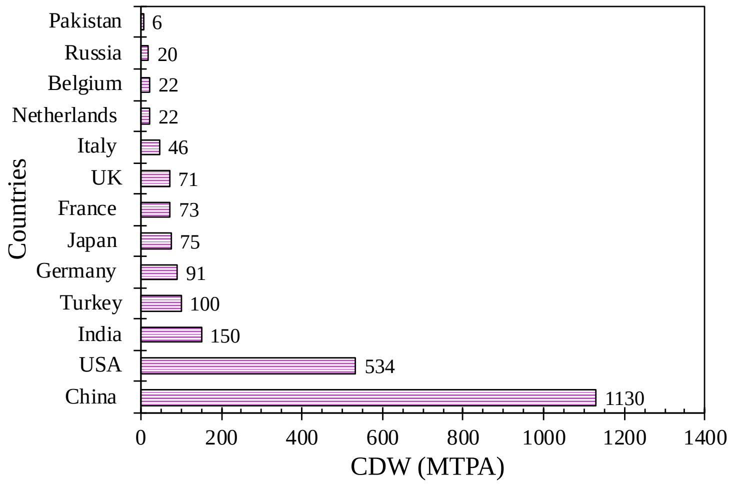

Fig. 1. CDW generation in populated countries (modified after Hoang et al. [4]; Haider et al. [5]; Pereira and Vieira [6]; Swarna et al. [7])

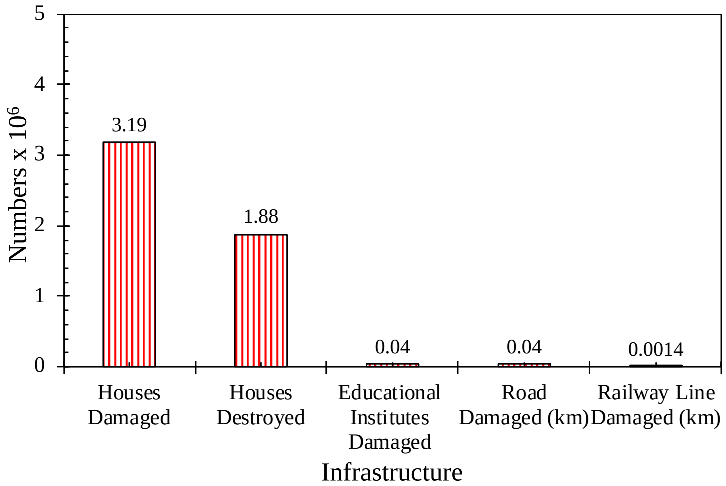

Fig. 2. Infrastructure damages during floods in 2010 and 2022 and earthquake in 2005 in Pakistan (modified after ADB [8])

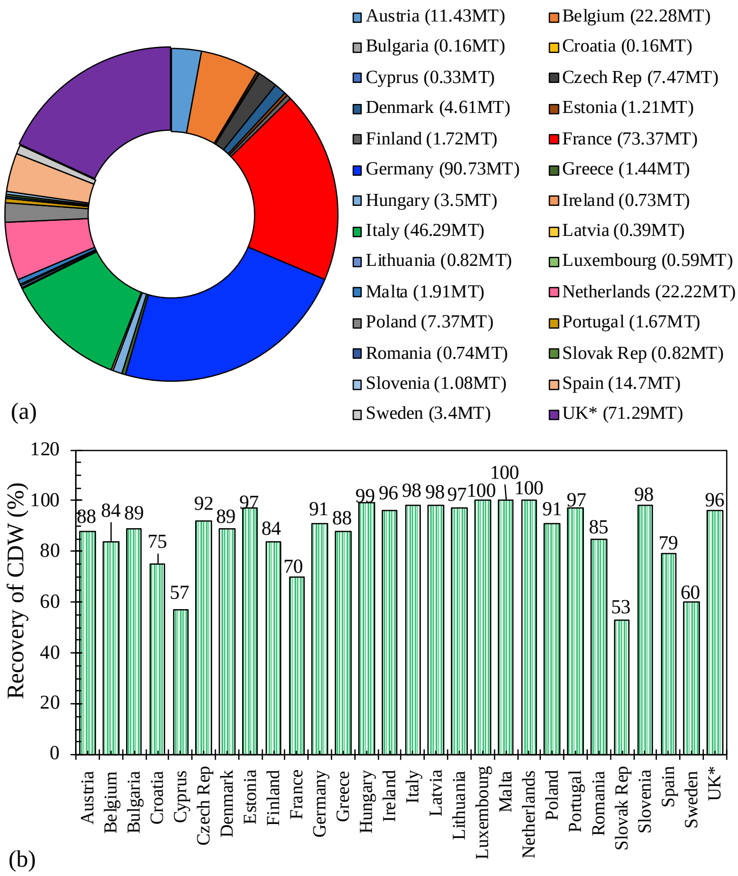

Fig. 3. (a) Annual CDW generation in EU; (b) Recovery of CDW in EU (modified after EEA [9])

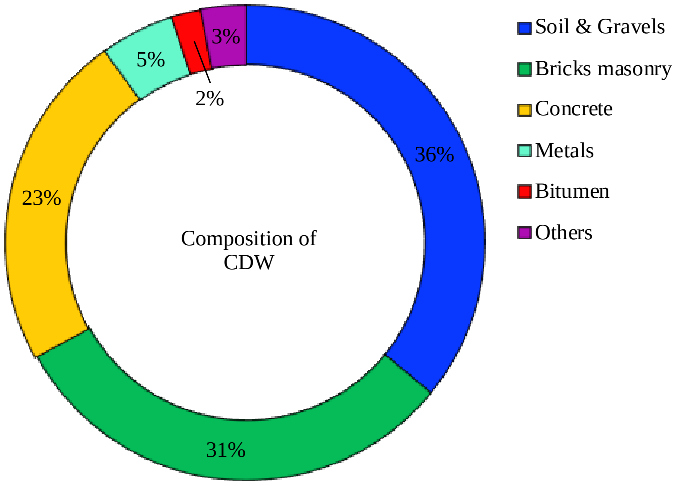

Fig. 4. Composition of CDW (modified after Mohammaddinia et al. [46])

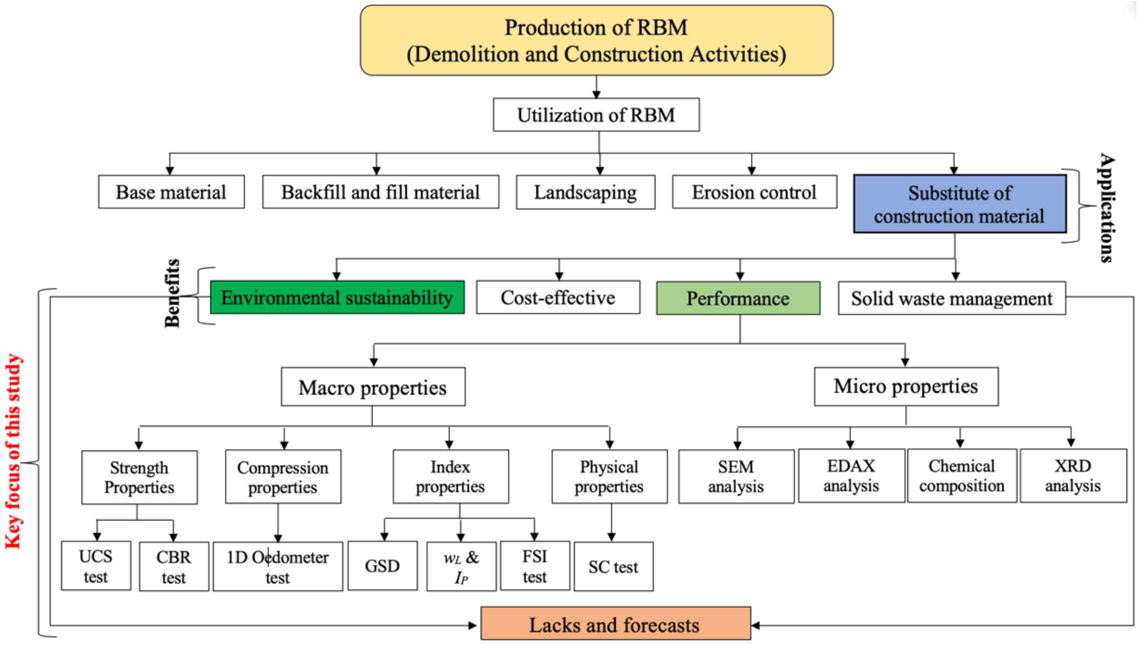

Fig. 5. Diagrammatical illustration of the scope of this study

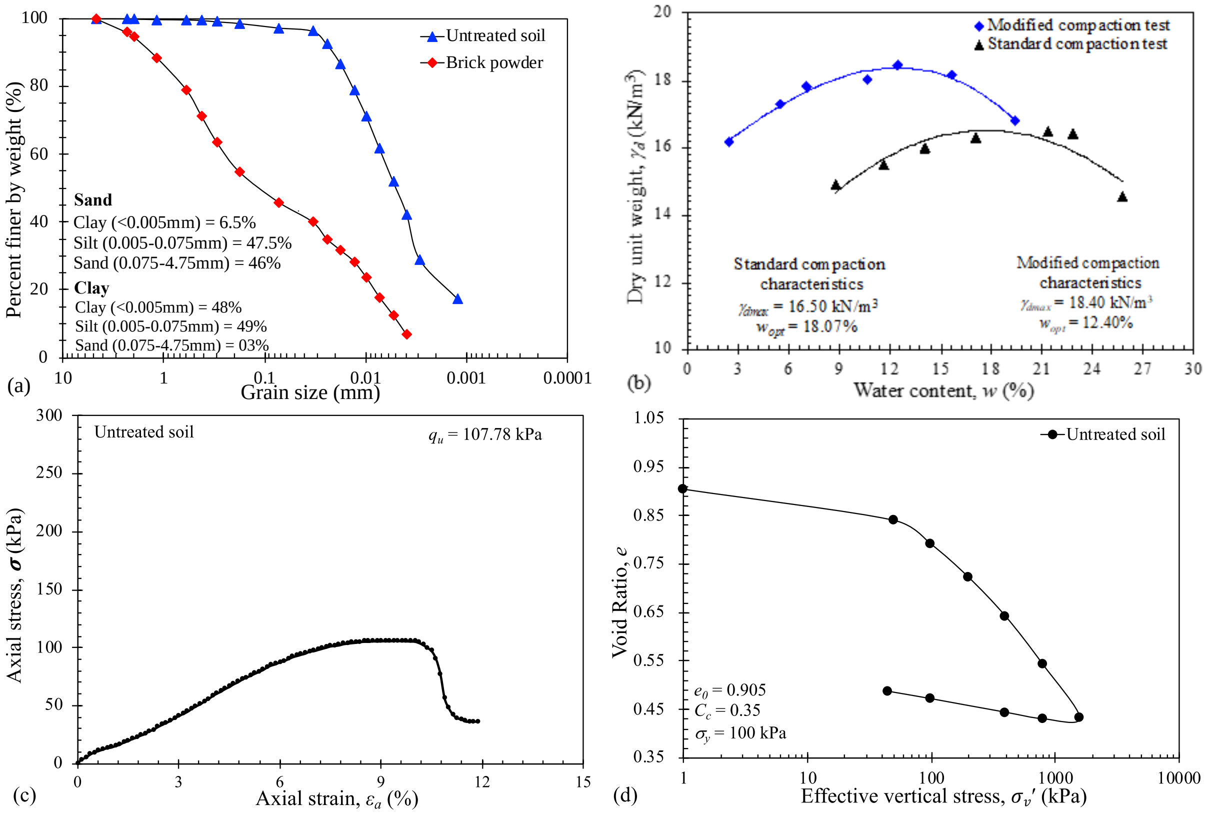

Fig. 6. Geotechnical characteristics of untreated specimen (a) grain size distribution curves; (b) compaction curves; (c) stress-strain curve; (d) compression curve

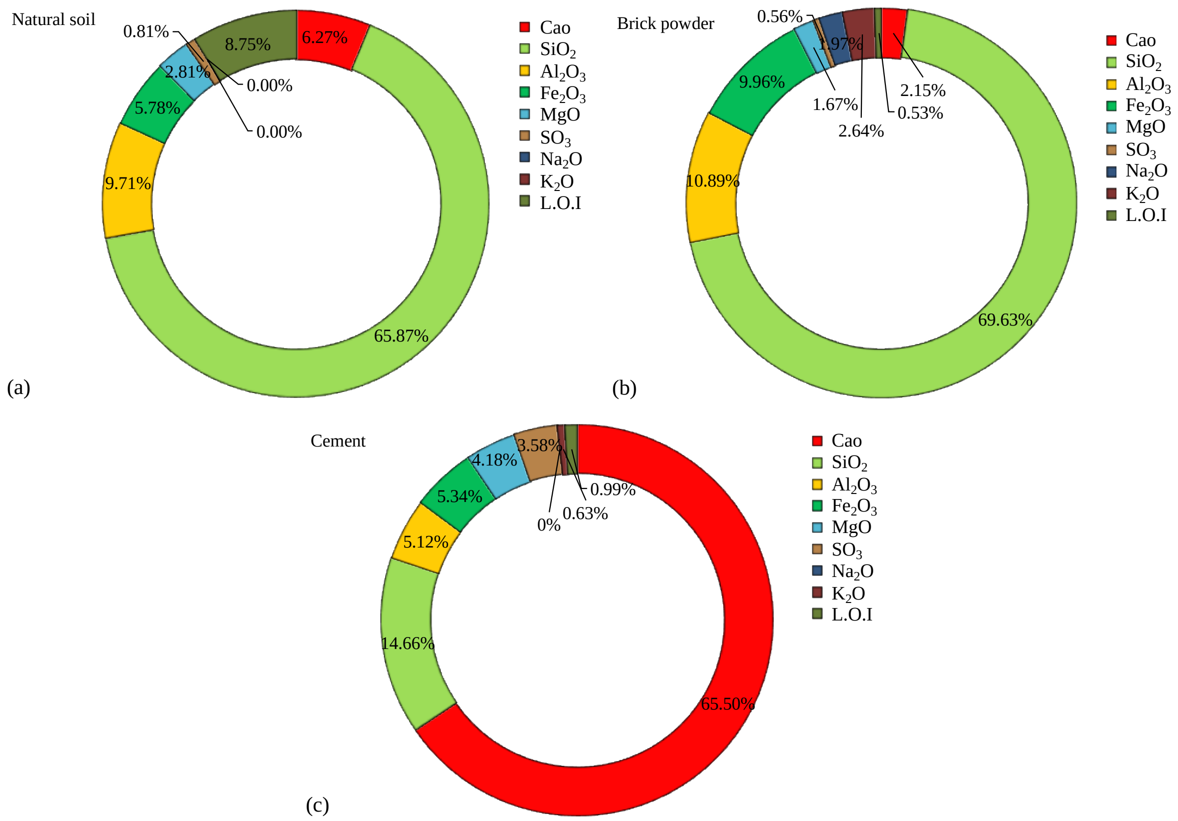

Fig. 7. Oxides composition of (a) natural soil; (b) brick powder; (c) cement

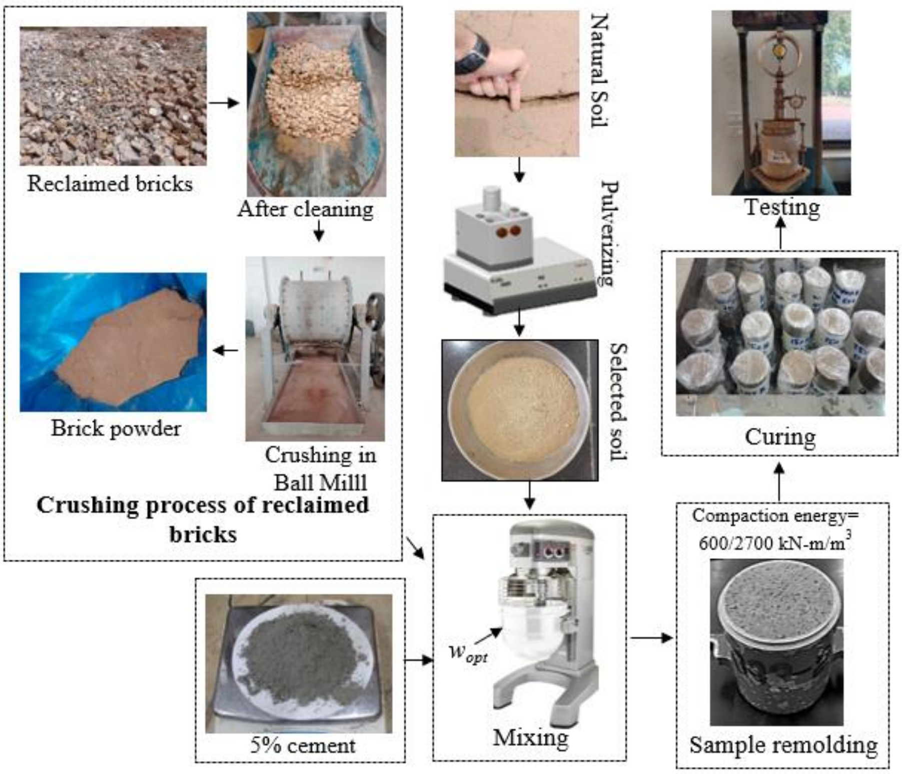

Fig. 8. Specimens preparation approach

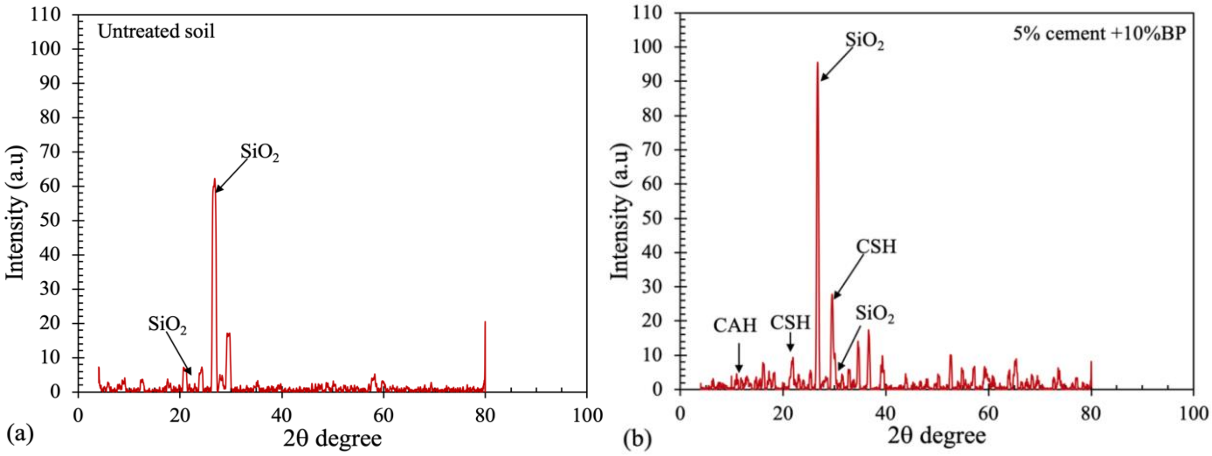

Fig. 9. XRD analyses of (a) untreated soil; (b) 5% cement+10% BP after 28 days of curing

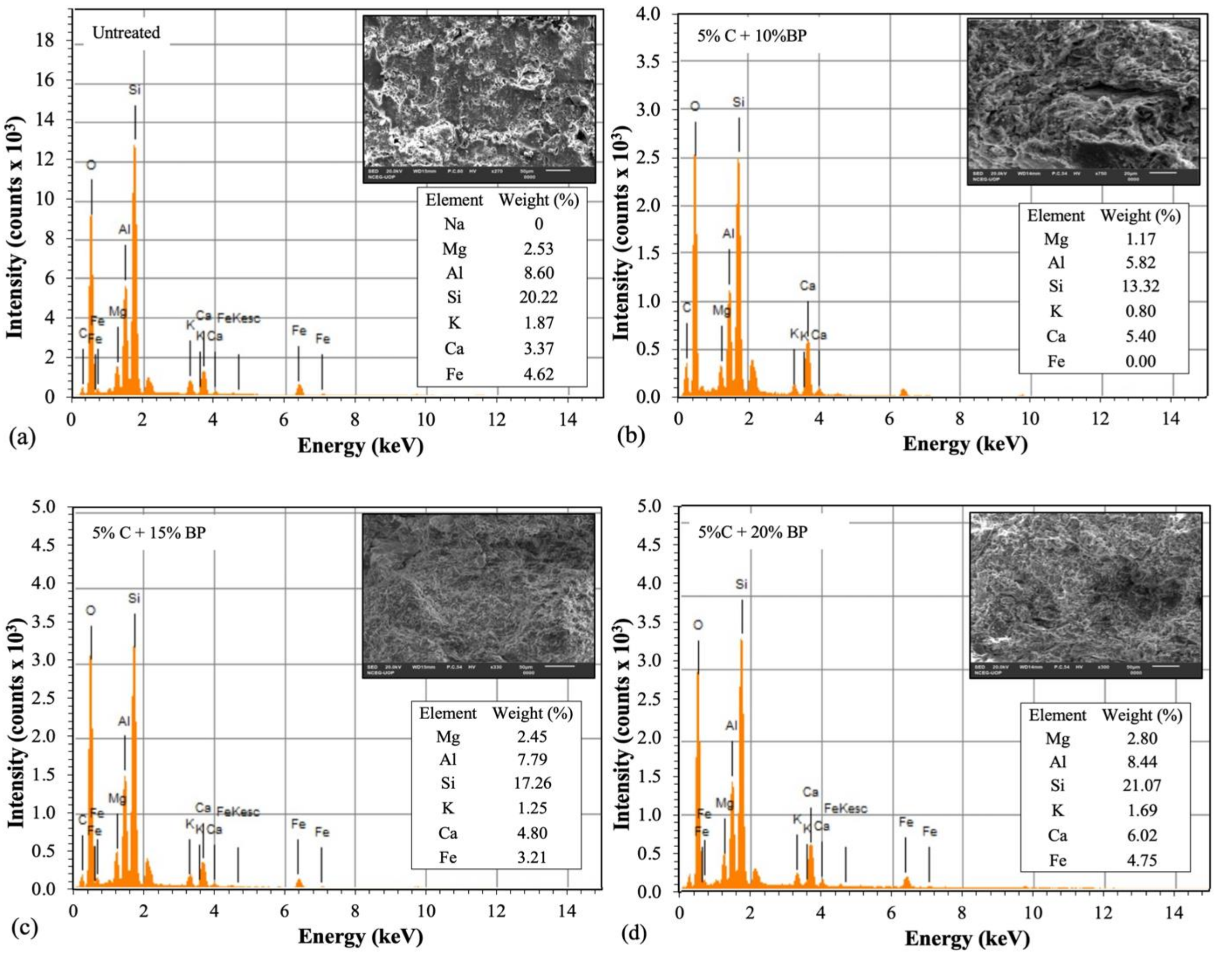

Fig. 10. EDAX analyses of 5% cement treated specimens at 28 days curing (a) untreated soil; (b) 10% BP; (c) 15% BP; (d) 20% BP

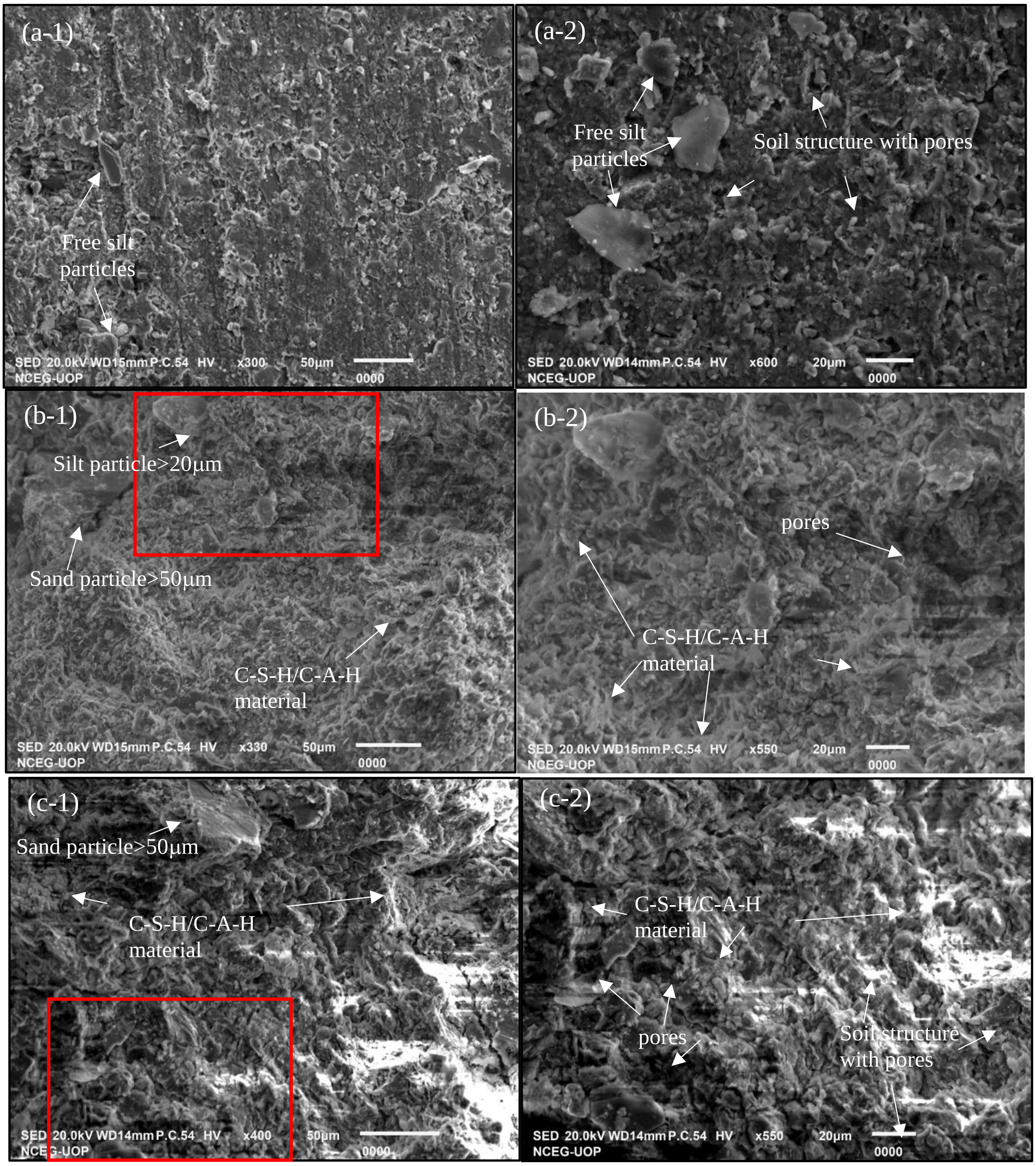

Fig. 11. SEM images of 5% cement treated specimens at 28 days curing (a) untreated soil; (b) 10% BP; (c) 15% BP

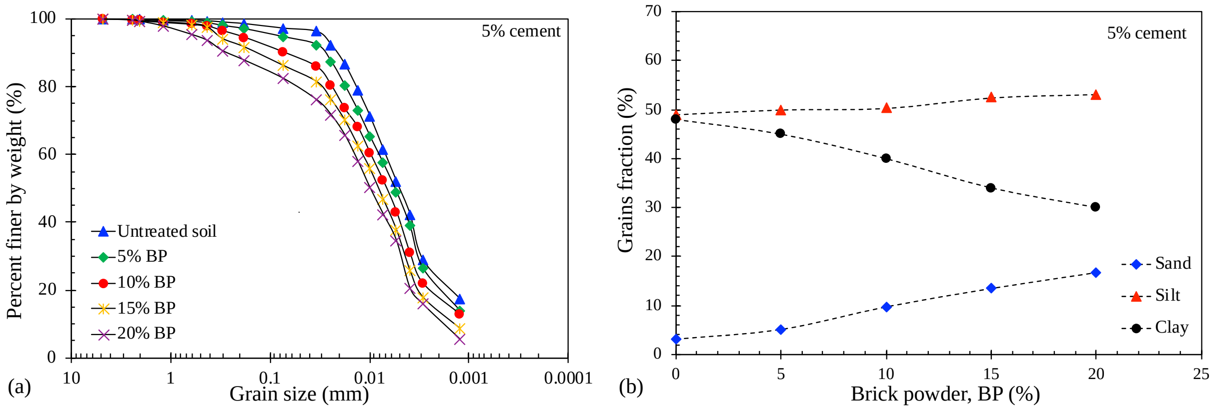

Fig. 12. Effect of cement and BP on (a) grain size distribution curves; (b) effect of BP on grains fraction

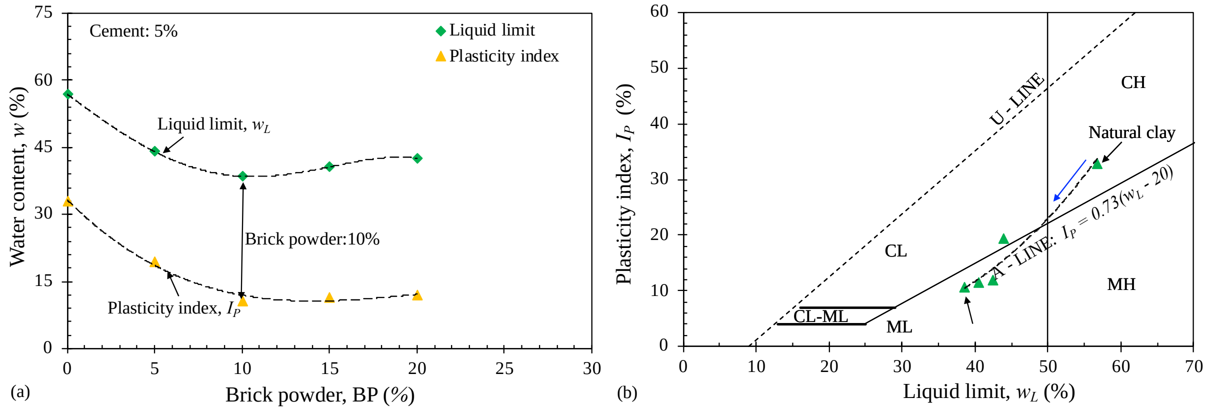

Fig. 13. Effect of cement and BP on (a) consistency limits; (b) w_L vs. I_P

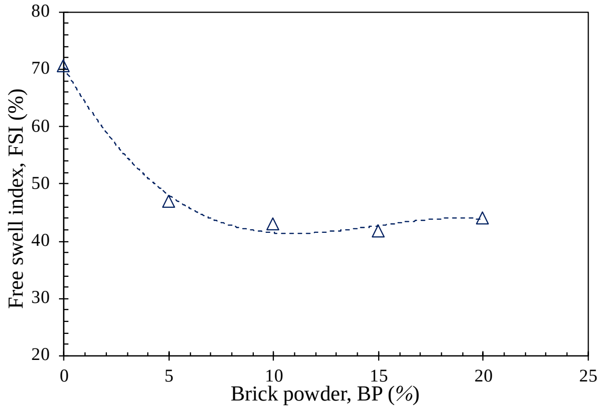

Fig. 14. Effect of cement and BP on FSI

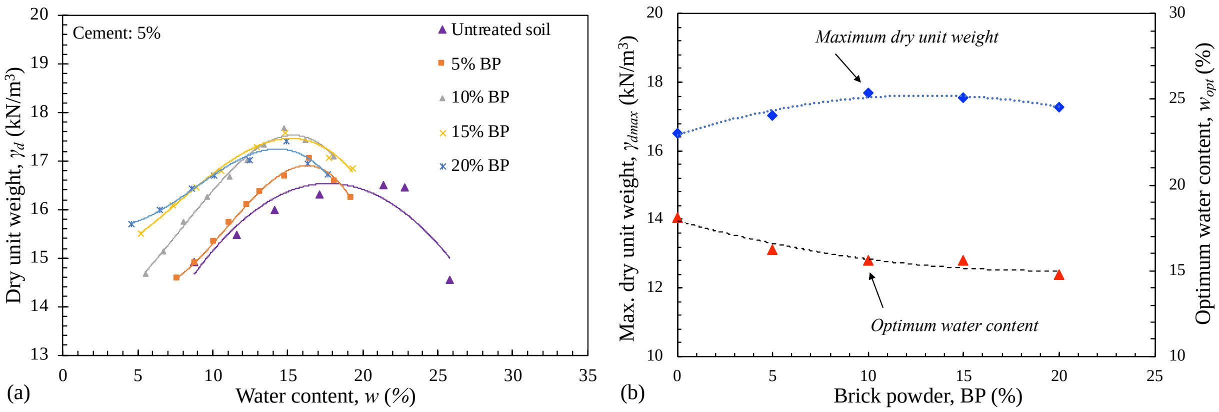

Fig. 15. Effect of cement and BP on (a) compaction curves; (b) γ_{dmax} and w_{opt}

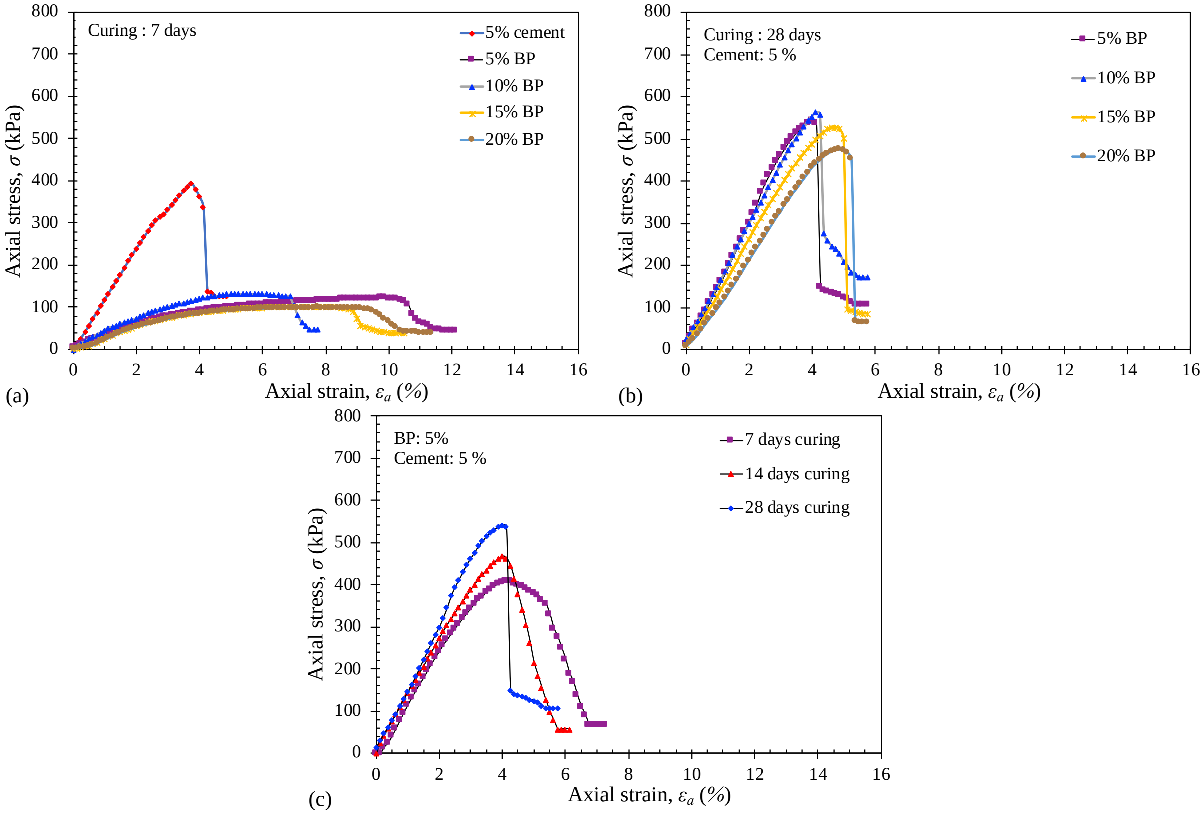

Fig. 16. Stress-strain curves of (a) cement and BP treated specimens; (b) effect of 5% cement+BP; (b) effect of curing

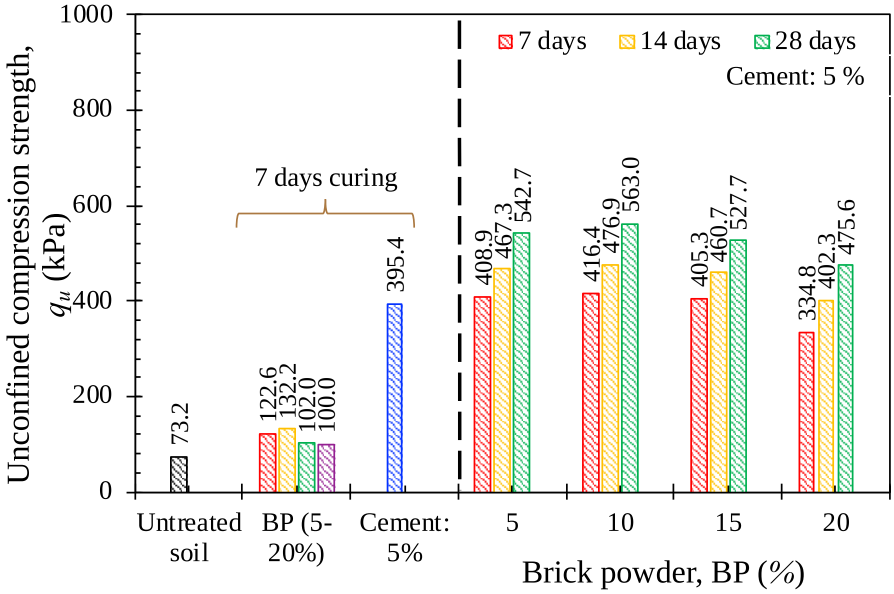

Fig. 17. Comparison of q_u of treated and untreated specimens

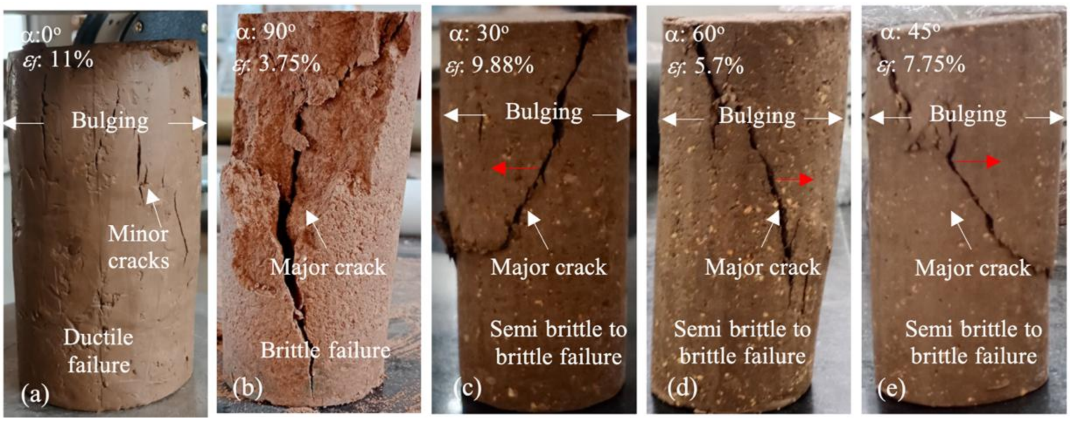

Fig. 18. Specimens failure morphology of (a) untreated; (b) 5% cement; (c) 5% BP; (d) 10% BP; (e) 20% BP

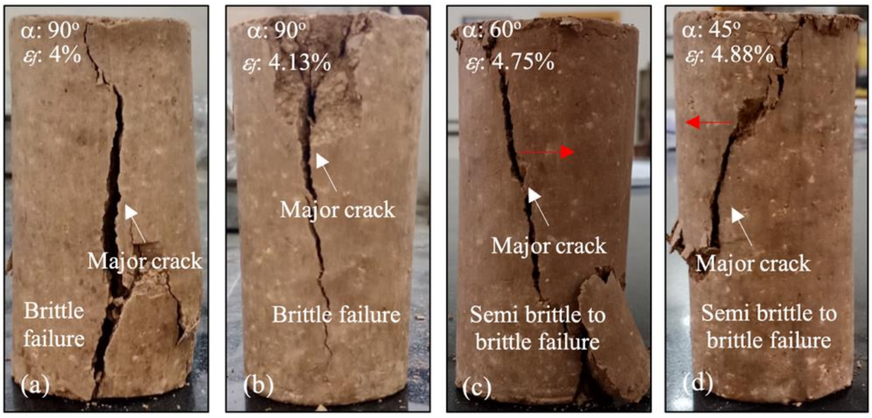

Fig. 19. Failure morphology of specimens treated with 5% cement and (a) 5% BP; (b) 10% BP; (c) 15% BP; (d) 20% BP, after 28 days of curing

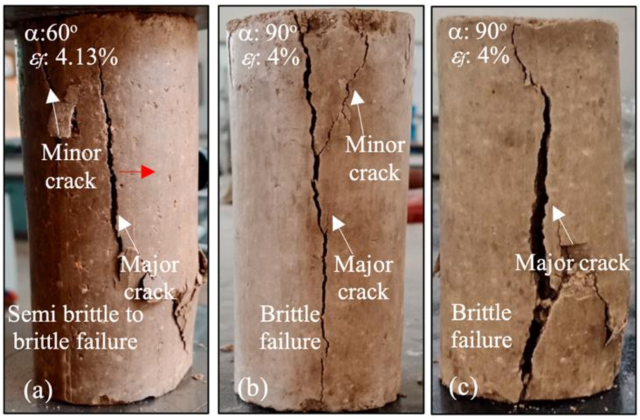

Fig. 20. Failure morphology of specimens treated with 5% cement and 5% BP (a) 7 days; (b) 14 days; (c) 28 days

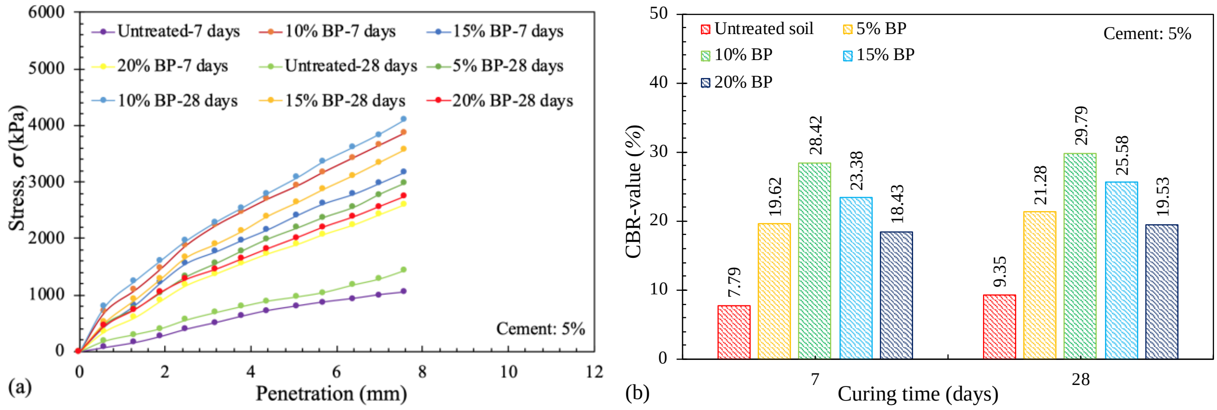

Fig. 21. CBR results (a) penetration vs σ curves; (b) effect of GFA and mellowing time; (c) effect of curing

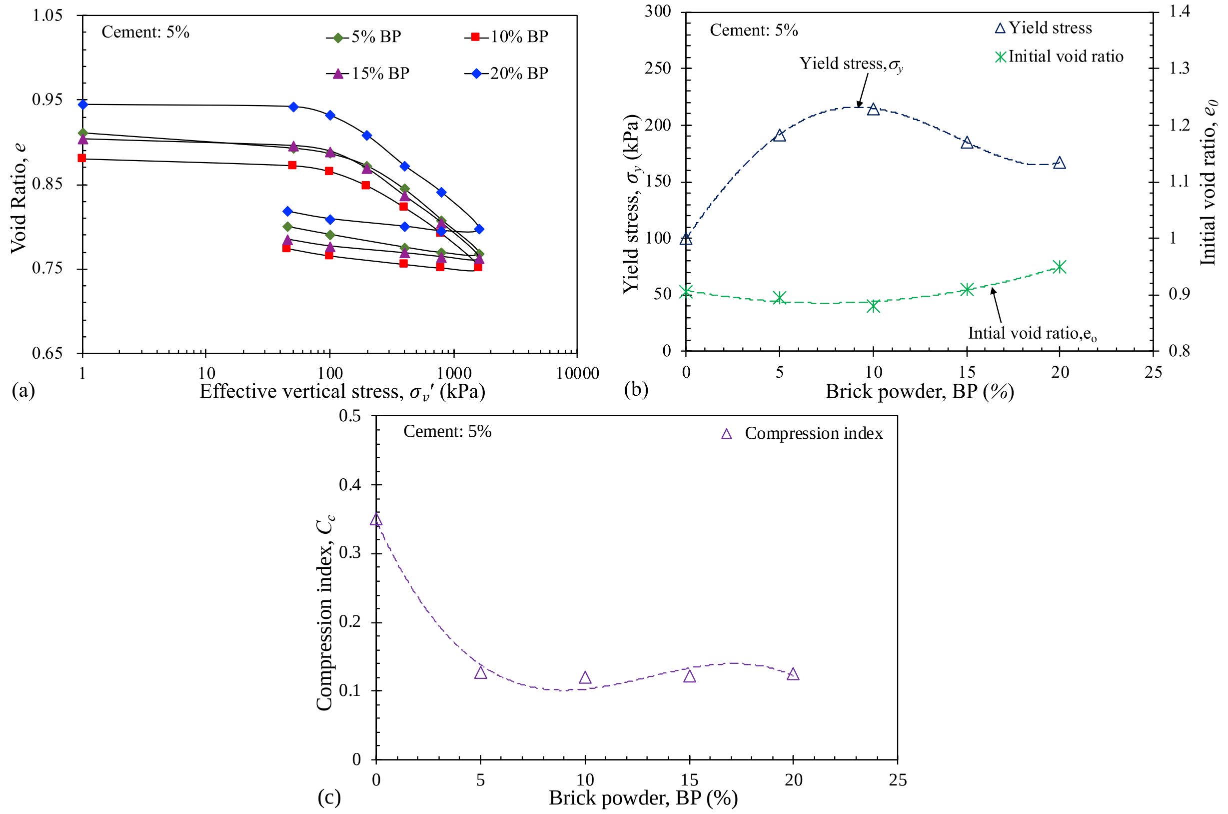

Fig. 22. Effect of cement and BP on (a) compression parameters (b) σ_y and e_0; (b) C_c, after 28 days of curing

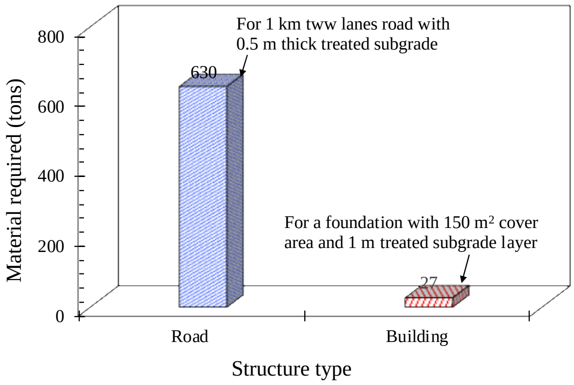

Fig. 23. CDW estimation for proposed soil improvement approach

Table

Table 1. Geotechnical properties of selected soil

Properties	Soil
Natural moisture content, w_n (%)	9.7
Specific gravity, G_s	2.71
Clay fraction (%)	48%
Silt fraction (%)	49%
Sand fraction (%)	3%
Liquid limit, w_L (%)	56.8
Plasticity Index, I_P (%)	33%
Maximum dry unit weight, γ_{dmax} (kN/m^3)	16.50
Optimum moisture content, w_{opt} (%)	18.07
Unsoaked California bearing ratio value (*CBR*-value)	7.79
Compression index, C_c	0.35
Initial void ratio, e_0	0.905
Yield stress, σ_y (kPa)	100
USCS Classification	CH

Table 2. Test matrix of this study

Analyses	Tests	Additives	Curing (days)
Micro properties	Chemical composition	Untreated, cement, brick powder	-
	X-ray Diffraction analysis	Untreated, 5% cement cum 10%BP	
	Scanning electron microscopy	Untreated, 5% cement cum 10% BP, 15% BP, 20% BP	28
	Energy-dispersive X-ray spectroscopy		
Macro properties	Sieve analysis and hydrometer analysis	Untreated, 5% cement cum 5%BP, 10% BP, 15% BP, 20% BP	-
	Consistency limits test		-
	Free swell index test		-
	Standard compaction test		-
	California bearing ratio test		28
	1D oedometer test		28
	Unconfined compression test	Untreated, 5% cement cum 5%BP, 10% BP, 15% BP, 20% BP	7, 14, 28
		5% cement, 5%BP, 10% BP, 15% BP, 20% BP	7